

AD-A270 124



PL-TR-91-2189

SIO Ref 91-15  
MPL-U-25/91

A SENSITIVITY STUDY OF DAYTIME VISIBILITY  
DETERMINATION WITH THE HORIZON SCANNING IMAGER

J. E. Shields  
R. W. Johnson  
M. E. Karr

University of California, San Diego  
Marine Physical Laboratory  
San Diego, CA 92152-6400

July 1991



Scientific Report No. 2

APPROVED FOR PUBLIC RELEASE; DISTRIBUTION UNLIMITED

93-20816



PHILLIPS LABORATORY  
AIR FORCE SYSTEMS COMMAND  
HANSCOM AIR FORCE BASE, MASSACHUSETTS 01731-5000

**Best  
Available  
Copy**

"This technical report has been reviewed and is approved for publication"

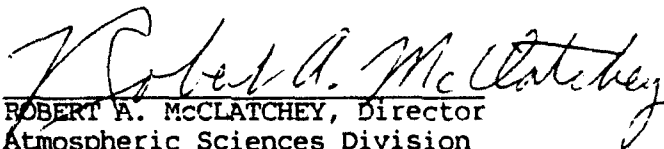


HENRY A. BROWN  
Contract Manager  
Atmospheric Structure Branch



DONALD D. GRANTHAM, Chief  
Atmospheric Structure Branch

FOR THE COMMANDER



ROBERT A. MCCLATCHEY, Director  
Atmospheric Sciences Division

This report has been reviewed by the ESD Public Affairs Office (PA) and is releasable to the National Technical Information Service (NTIS).

Qualified requestors may obtain additional copies from the Defense Technical Information Center.

If your address has changed, or if you wish to be removed from the mailing list, or if the addressee is no longer employed by your organization, please notify PL/IMA, Hanscom AFB, MA 01731-5000. This will assist us in maintaining a current mailing list.

Do not return copies of this report unless contractual obligations or notices on a specific document requires that it be returned.

REPORT DOCUMENTATION PAGE			Form Approved OMB No. 0704-0188	
<small>Public reporting burden for this collection of information is estimated to average 1 hour per response, including the time for reviewing instructions, searching existing data sources, gathering and maintaining the data needed, and completing and reviewing the collection of information. Send comments regarding this burden estimate or any other aspect of this collection of information, including suggestions for reducing this burden, to Washington Headquarters Services, Directorate for Information Operations and Reports, 1215 Jefferson Davis Highway, Suite 1204, Arlington, VA 22202-4302, and to the Office of Management and Budget, Paperwork Reduction Project (0704-188), Washington, DC 20503.</small>				
1. Agency Use Only (Leave blank).		2. Report Date. July 1991		3. Report Type and Dates Covered. Scientific No. 2
4. Title and Subtitle.  A Sensitivity Study of Daytime Visibility Determination With The Horizon Scanning Imager			5. Funding Numbers. Program Element No. F19628-88-C-0154 63707F Project No. 2688 Task No. 03 Accession No. HA	
6. Author(s). J. E. Shields R. W. Johnson M. E. Karr				
7. Performing Organization Name(s) and Address(es).  University of California, San Diego Marine Physical Laboratory San Diego, CA 92093-0701			8. Performing Organization Report Number.  SIO Ref 91-15  MPL-U-25/91	
9. Sponsoring/Monitoring Agency Name(s) and Address(es). Philips Laboratory Hanscom AFB, MA 01731-5000  Contract Manager: Dr. H. A. Brown/LYA			10. Sponsoring/Monitoring Agency Report Number.  PL-TR-91-2189	
11. Supplementary Notes.				
12a. Distribution/Availability Statement.  Approved for public release, distribution unlimited.			12b. Distribution Code.	
13. Abstract (Maximum 200 words).  The Horizon Scanning Imager is an automated imaging system for determination of visibility during the daytime. This is accomplished through evaluation of contrast transmission of the atmosphere, which is determined from the measured radiance of dark targets near the horizon. The determination of visibility during the daytime by the Horizon Scanning Imager is influenced by a number of parameters, some measured and others input by the operator. These include the measured target radiance, measured horizon radiance, and inherent contrast of the target with respect to the horizon. This report contains a sensitivity study, in which the impact of uncertainty in these parameters is determined. On the basis of this study, specific recommendations are made to improve the visibility determinations. The first set of recommendations relates to the sensor accuracy and includes ways to improve the measurements and also ways to mitigate the impact of the residual errors. The second set of recommendations details strategies to minimize the impact of non-ideal measurement conditions.				
14. Subject Terms. Visibility, Contrast Transmittance, Atmosphere, Sector Visibility, Weather Sensors, Aviation Weather Observations, Weather, Atmospheric Visibility			15. Number of Pages. 46	
			16. Price Code.	
17. Security Classification of Report. Unclassified	18. Security Classification of This Page. Unclassified	19. Security Classification of Abstract. Unclassified	20. Limitation of Abstract. SAR	

## SUMMARY

The Horizon Scanning Imager is an automated imaging system for determination of visibility during the daytime. This is accomplished through evaluation of contrast transmission of the atmosphere, which is determined from the measured radiance of dark targets near the horizon. The determination of visibility during the daytime by the Horizon Scanning Imager is influenced by a number of parameters, some measured and others input by the operator. These include the measured target radiance, measured horizon radiance, and inherent contrast of the target with respect to the horizon. This report contains a sensitivity study, in which the impact of uncertainty in these parameters is determined. On the basis of this study, specific recommendations are made to improve the visibility determinations. The first set of recommendations relates to the sensor accuracy and includes ways to improve the measurements and also ways to mitigate the impact of the residual errors. The second set of recommendations details strategies to minimize the impact of non-ideal measurement conditions.

DTIC QUALITY INSPECTED 1

Accession For	
NTIS GRA&I	<input checked="" type="checkbox"/>
DTIC TAB	<input type="checkbox"/>
Unannounced	<input type="checkbox"/>
Justification	
By _____	
Distribution/	
Availability Codes	
<div style="display: flex; justify-content: space-between;"> <span>Dist:</span> <span style="font-size: 2em; font-family: cursive;">A-1</span> </div>	<div style="display: flex; justify-content: space-between;"> <span>Avail and/or</span> <span>Special</span> </div>

## TABLE OF CONTENTS

Summary .....	iii
List of Illustrations .....	vii
1.0 Introduction .....	1
2.0 Sensitivity to Inherent Contrast Values .....	1
2.1 Computation and Interpretation of the $C_0$ Sensitivity Plots .....	2
2.2 Results of the $C_0$ Sensitivity Computations .....	7
3.0 Sensitivity to Measured Target Uncertainties .....	9
3.1 Computation of Sensitivity to Measured Target Uncertainties .....	9
3.2 Evaluation of Sensitivity to Measured Target Uncertainties .....	10
4.0 Sensitivity to Measured Horizon Brightness Uncertainties .....	15
4.1 Computation of Sensitivity to Measured Horizon Uncertainties .....	15
4.2 Evaluation of Sensitivity to Measured Horizon Uncertainties .....	20
5.0 Sensitivity to Non-linearity of Camera Response .....	20
5.1 Computation of Sensitivity to Measured Non-linearity .....	20
5.2 Evaluation of Sensitivity to Measured Non-linearity .....	21
5.3 Characterization and Stability of System Response; Implications .....	28
6.0 Sensitivity to Target Range and Contrast Threshold .....	32
6.1 Sensitivity to Target Range .....	32
6.2 Sensitivity to Contrast Threshold .....	32
7.0 Summary .....	33
8.0 Recommendations .....	33
8.1 Improvements Relating to Measurement Accuracy .....	36
8.2 Improvements Relating to Non-ideal Conditions .....	37
9.0 Conclusion .....	37
10.0 Acknowledgements .....	38
11.0 References .....	38

## LIST OF ILLUSTRATIONS

Test 1a	Sensitivity of Derived Visibility to an error in input $C_0$ when the actual $C_0$ is .8 . . . . .	3
Test 1b	Sensitivity of Derived Visibility to an error in input $C_0$ when the actual $C_0$ is .5 . . . . .	4
Test 1c	Sensitivity of Derived Visibility to a variation in actual $C_0$ when a fixed input $C_0$ of .8 is used . . . . .	5
Test 1d	Sensitivity of Derived Visibility to a variation in actual $C_0$ when a fixed input $C_0$ of .5 is used . . . . .	6
Test 2a	Sensitivity of Derived Visibility to Measured Target Radiance Uncertainty, $C_0 = .8$ , $L_q = 100$ . . . . .	11
Test 2b	Sensitivity of Derived Visibility to Measured Target Radiance Uncertainty, $C_0 = .8$ , $L_q = 200$ . . . . .	12
Test 2c	Sensitivity of Derived Visibility to Measured Target Radiance Uncertainty, $C_0 = .5$ , $L_q = 100$ . . . . .	13
Test 2d	Sensitivity of Derived Visibility to Measured Target Radiance Uncertainty, $C_0 = .5$ , $L_q = 200$ . . . . .	14
Test 3a	Sensitivity of Derived Visibility to Measured Horizon Radiance Uncertainty, $C_0 = .8$ , $L_q = 100$ . . . . .	16
Test 3b	Sensitivity of Derived Visibility to Measured Horizon Radiance Uncertainty, $C_0 = .8$ , $L_q = 200$ . . . . .	17
Test 3c	Sensitivity of Derived Visibility to Measured Horizon Radiance Uncertainty, $C_0 = .5$ , $L_q = 100$ . . . . .	18
Test 3d	Sensitivity of Derived Visibility to Measured Horizon Radiance Uncertainty, $C_0 = .5$ , $L_q = 200$ . . . . .	19
Test 4a	Sensitivity of Derived Visibility to Non-Linearities in Camera Response, $C_0 = .8$ , $L_q = 100$ . . . . .	22
Test 4b	Sensitivity of Derived Visibility to Non-Linearities in Camera Response, $C_0 = .8$ , $L_q = 200$ . . . . .	23
Test 4c	Sensitivity of Derived Visibility to Non-Linearities in Camera Response, $C_0 = .8$ , $L_q = 220$ . . . . .	24
Test 4d	Sensitivity of Derived Visibility to Non-Linearities in Camera Response, $C_0 = .5$ , $L_q = 100$ . . . . .	25
Test 4e	Sensitivity of Derived Visibility to Non-Linearities in Camera Response, $C_0 = .5$ , $L_q = 200$ . . . . .	26
Test 4f	Sensitivity of Derived Visibility to Non-Linearities in Camera Response, $C_0 = .5$ , $L_q = 220$ . . . . .	27

Test 5a	Sensitivity of Derived Visibility to Precision and Stability of Non-Linearity, $C_0 = .8$ , $L_q = 100$ . . . . .	29
Test 5b	Sensitivity of Derived Visibility to Precision and Stability of Non-Linearity, $C_0 = .8$ , $L_q = 200$ . . . . .	30
Test 5c	Sensitivity of Derived Visibility to Precision and Stability of Non-Linearity, $C_0 = .8$ , $L_q = 220$ . . . . .	31
Summary a	Summary for $C_0 = .8$ , $L_q = 200$ . . . . .	34
Summary b	Summary for $C_0 = .5$ , $L_q = 200$ . . . . .	35



## 1.0 INTRODUCTION

The determination of visibility during the daytime by the Horizon Scanning Imager (HSI) (Johnson et al, 1990) is influenced by a number of parameters, both measured and input. The system works essentially through measurement of the relative radiance of dark targets and the horizon sky, as explained in Johnson et al, 1989. These measurements are made for several targets in each of several azimuthal directions around the horizon. An apparent contrast of the target with respect to the sky can be computed directly from the measured radiances. Then the visibility can be determined from the apparent contrast, if the inherent contrast of the target with respect to the sky, and the range to the target, are known.

An early study of the impact of various theoretical uncertainties is included in Johnson et al, 1989. In this early study, the impact of uncertain inherent contrast, and overcast or partly cloudy horizon sky conditions were considered. This current note extends the study of the impact of inherent contrast uncertainties, and also evaluates the impact of measurement uncertainties. In particular, it is important to note which of the problem areas can be readily controlled, and which represent basic limitations to the accuracy of the device.

This note will discuss specifically the sensitivity of visibility determinations to errors in input  $C_0$ , measured target relative radiance, measured horizon relative radiance, camera linearity, and input target range. Each section first discusses how the sensitivity plots for the given parameter were derived. (Numeric examples are given in some cases.) This is followed by a discussion of the results implied by the plots. Each section then includes a discussion of the potential sources of these uncertainties, and potential means of minimizing the uncertainties.

## 2.0 SENSITIVITY TO INHERENT CONTRAST VALUES

The inherent contrast is defined by

$$C_o = \frac{tL_o - bL_o}{bL_o} \quad 2.1$$

where  $tL_o$  is the inherent target radiance, and  $bL_o$  is the inherent background radiance. Note that the word "inherent" signifies that the radiance is measured from a distance of 0. Also note that if the target is black,  $tL_o$  is equal to 0, and the inherent contrast stays fixed at -1, even if the background radiance changes.

The HSI system does not measure  $C_0$ ; this value is an input set by the user. The visibility is then computed from the equation

$$\frac{V}{r} = \ln \left( \frac{\epsilon}{C_r} \right) / \ln \left( \frac{C_r}{C_o} \right) \quad 2.2$$

where  $r$  is range to the target, and  $\epsilon$  is the human contrast threshold associated with the definition of visibility.  $C_r$  is the measured contrast, or the contrast at range  $r$ , defined by

$$C_r = \frac{tL_r - bL_r}{bL_r} \quad , \quad 2.3$$

where  $tL_r$  and  $bL_r$  are the target and background radiances, respectively, at range  $r$ . For a full discussion of these terms, see Duntley, 1957.

Equation 2.2 is the primary expression utilized by the HSI to derive visibility from the measured contrast. This equation is derived in Johnson et al, 1989. The derivation assumes that the contrast with respect to the horizon sky is used, and the horizon sky radiance approximates the equilibrium radiance ( $L_q$ ), defined in Johnson et al 1989, and earlier references. A threshold  $\epsilon$  of .05 is normally used in the HSI; this is the value of human contrast threshold associated with the definition of visibility (ref. Douglas & Booker, 1977).

There are a variety of philosophical approaches to determining visibility with a system such as the HSI. The human observer using non-ideal visual targets will make visibility assessments which are not strictly in accordance with the classically defined visibility. The HSI can simulate this human bias or not, according to the needs of the application, through appropriate changes to Eq. 2.2. Whereas these changes would affect the magnitude of the determined visibility to a limited degree, they have little impact on the results of the sensitivity study contained herein.

It should also be noted that although  $C_0$  values are negative for dark targets, the human visual response depends on the absolute magnitude of  $C_0$ ; therefore positive  $C_0$  values have been used in most of our reports, for ease of presentation. In this note, the negative sign must be kept in some of the internal computations used to generate the plots, however the positive sign has been used in presenting the results, for consistency with earlier work.

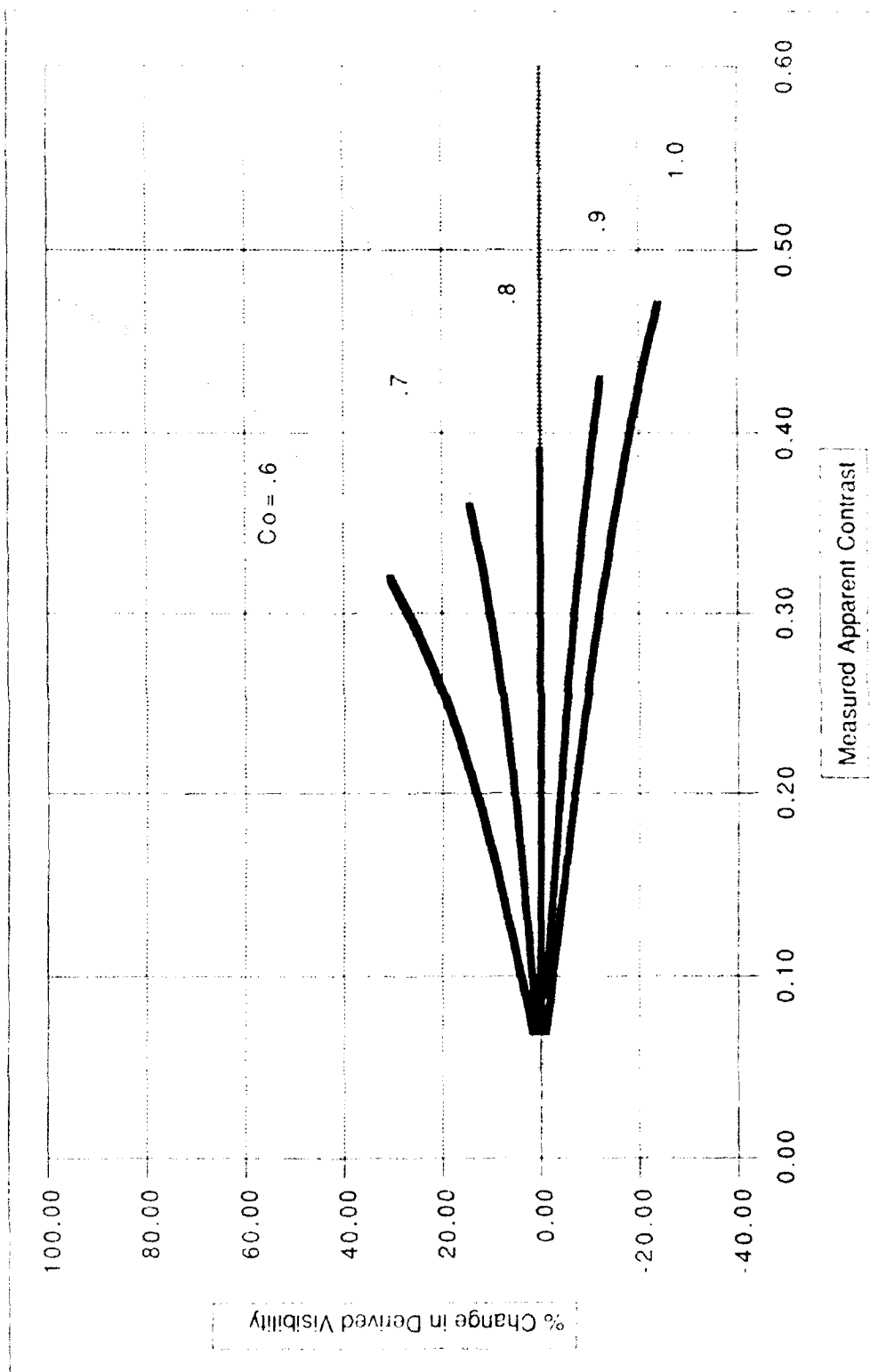
## 2.1 Computation and Interpretation of the $C_0$ Sensitivity Plots

The sensitivity of the derived visibility to uncertainties in the inherent contrast is illustrated by a series of four plots, labeled "Test 1a" through "Test 1d". The first plot, labeled Test 1a, shows the sensitivity of derived visibility to changes in input  $C_0$  when the actual  $C_0$  value is 0.8. That is, if we are measuring a target which has an inherent contrast of -0.8 with respect to the sky, but we input some other value, what is the error in derived visibility due to this input error. The visibility we would derive is given by Eq. 2.2 using the input  $C_0$ ; the visibility we should have derived, given the correct  $C_0$  value, is given by Eq. 2.2 with a  $C_0$  of 0.8 input.

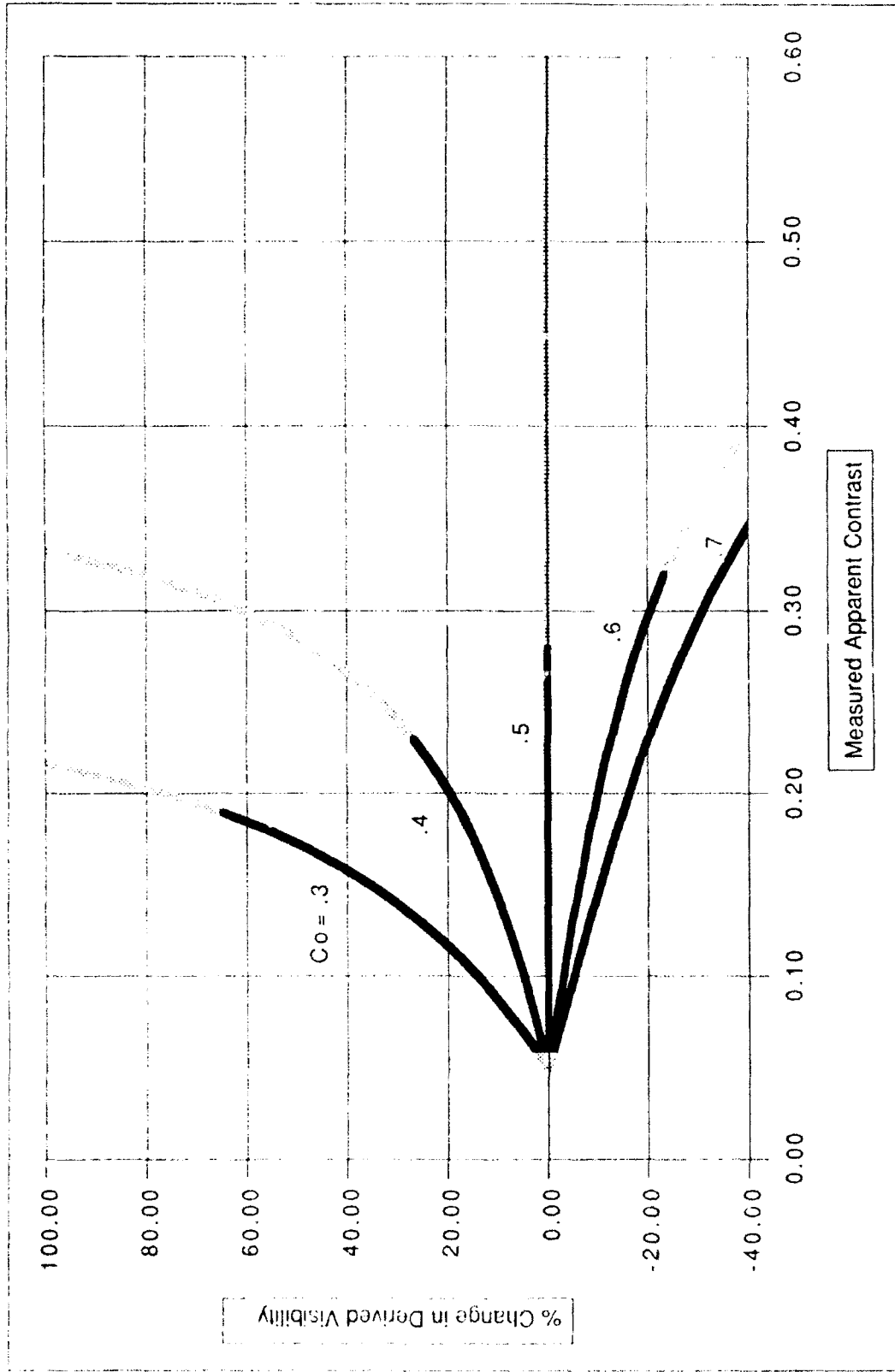
Thus to determine the error in the derived visibility, one first computes visibility using the input  $C_0$  value and Eq. 2.2, then divides this by the visibility computed using a  $C_0$  value of 0.8. For example, if a target at range 10 miles has an apparent contrast  $C_r$  value of 0.2, and the correct  $C_0$  is 0.8, the derived visibility found using Eq. 2.2 should be 20 miles. An input  $C_0$  value of 0.6 would yield a derived visibility of 22.6 miles, for an error of 13%.

The error is computed for a range of input  $C_r$  and  $C_0$  values. Note that the error does not depend on the input range ( $r$ ) value, and the input  $\epsilon$  value is not normally varied; thus these variables do not impact the assessment of the error due to  $C_0$  uncertainty.

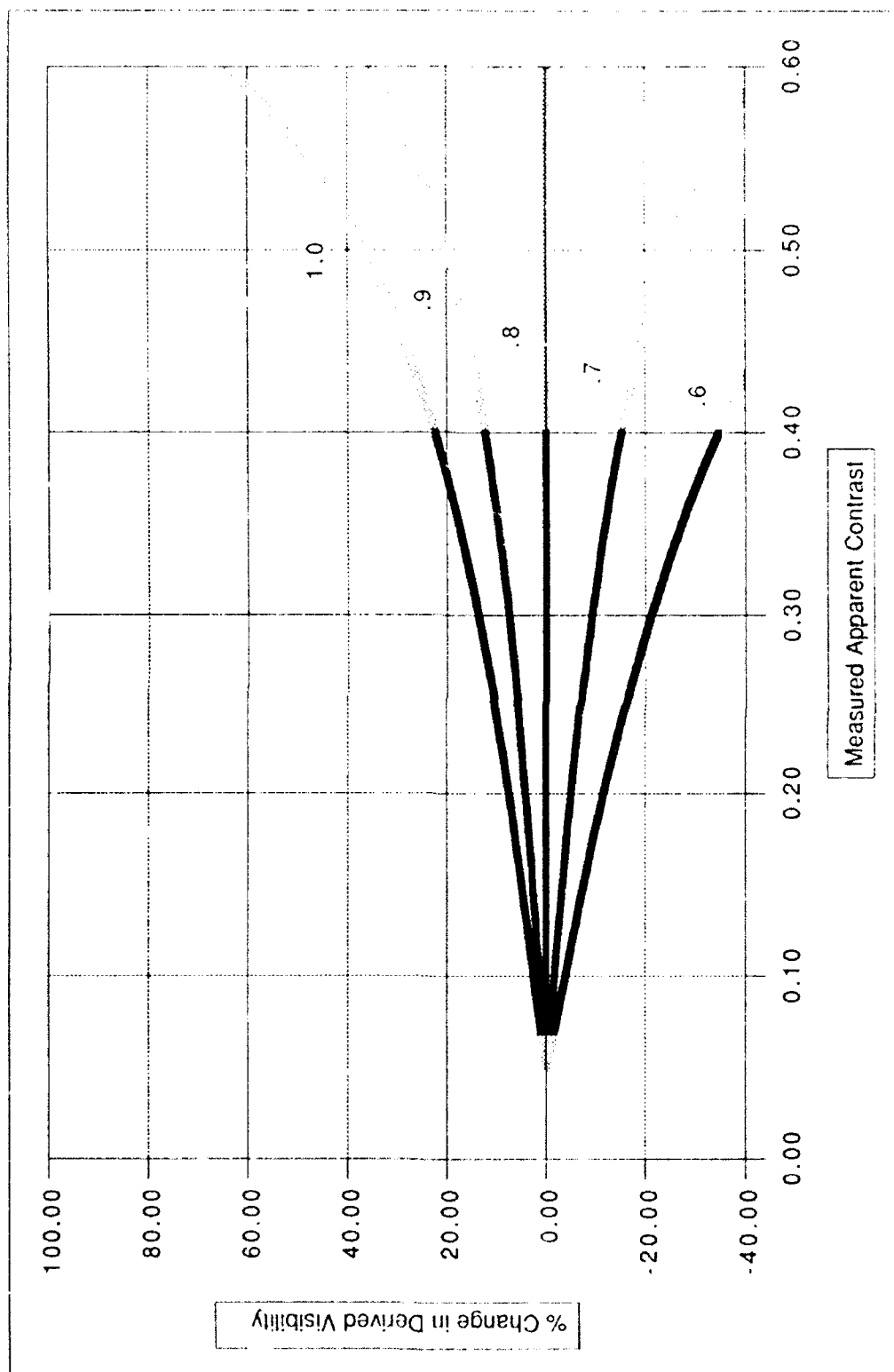
In the Test 1a plot, the uncertainty is plotted as a function of measured apparent contrast  $C_r$ . Note that when  $C_r$  is close to .05, the error approaches 0. Physically, this occurs when the target is at a range about equal to the visibility; that is, the apparent



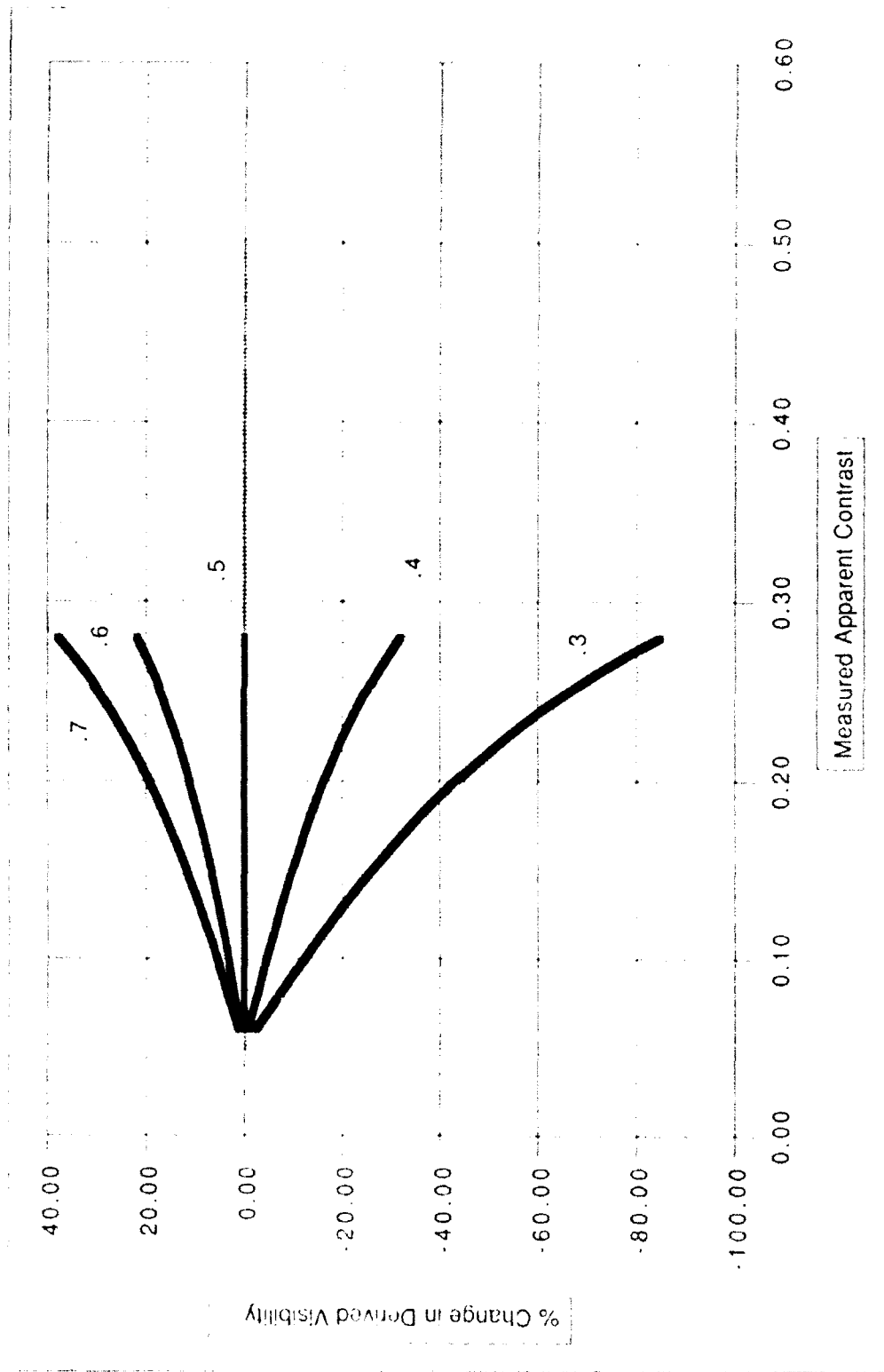
Test 1a Sensitivity of Derived Visibility to an error in input  $C_o$  when the actual  $C_o$  is .8



**Test 1 b** Sensitivity of Derived Visibility to an error in input  $C_o$  when the actual  $C_o$  is .5



**Test 1c** Sensitivity of Derived Visibility to a variation in actual Contrast when a fixed input Contrast of .8 is used



**Test 1d** Sensitivity of Derived Visibility to a variation in actual Co when a fixed input Co of .5 is used

contrast approaches the visual threshold of .05 when the target range is close to the visibility. Thus the plot may be interpreted as showing that the error due to uncertainty in  $C_0$  is quite small if the target range is similar to the visibility, and becomes larger as the target range becomes significantly less than the visibility.

The HSI algorithm has two automatic cutoff values. When  $V/r$  is less than 1.15 or greater than 4.0, the visibility value is given a "greater than" or "less than" value. In Test 1a, the curves are plotted in black (solid lines) where the  $V/r$  values lie within this range and the derived visibility values are used; the portions of the curve which are grey show where  $V/r$  values are outside the bounds. For example, if a  $C_0$  value of .6 is input, the  $V/r$  cutoff occurs at a measured  $C_r$  value of .32, and the maximum error is about 30%. The grey curves show what the error would be, if the possible  $C_r$  range were changed due to a change in the  $V/r$  cutoffs.

Test 1b shows the sensitivity of visibility to  $C_0$  input errors, if the actual  $C_0$  is .5. The values of .8 and .5 for actual  $C_0$  were chosen for tests 1a and 1b, because they are close to the normal bounds we might expect to use. A  $C_0$  of .8 is perhaps typical of the blackest targets we can expect to find among targets of opportunity; a  $C_0$  value of .5 was chosen to represent a significantly non-ideal (non-black) target.

Test 1b shows similar characteristics to Test 1a, in the sense that the error in determined visibility due to the uncertainty in the  $C_0$  value is vanishingly small for targets at range equal to visibility. The error increases as the target range becomes smaller, and measured apparent contrasts become larger. The errors become quite large at the maximum  $C_r$  values, indicating a certain risk associated with using non-ideal targets.

The third and fourth plots, Tests 1c and 1d, show the impact of  $C_0$  uncertainties in a slightly different way. These plots show the resulting error if a fixed input value is used, but the actual inherent contrast of the target with respect to the horizon sky changes. ( $C_0$  can change because of the impact of changing lighting conditions on the target radiance; it is also impacted by changes in the horizon radiance. The equilibrium radiance, and therefore horizon radiance, is highly dependent on the path-of-sight's scattering angle with respect to the sun.) For an example of the impact of changes in  $C_0$ , consider the case above where the visibility is 20 miles, and the range 10 miles. If  $C_0$  is really .6, it can be derived from Eq. 2.2 that  $C_r$  must have been .1732. Then if we measure  $C_r = .1732$ , and input a  $C_0$  value of .8, we will derive a visibility value of 18.1 miles, for a -9.4% error.

It should be noted that in Test 1c, the  $V/r$  cutoffs all occur at the same value of  $C_r$ . Looking at Eq. 2.2, one can see that if  $C_0$  and  $\epsilon$  are fixed,  $V/r$  will be directly related to  $C_r$ . The HSI algorithm must compute  $V/r$  using its input value of  $C_0$ . In Tests 1c and 1d, that input  $C_0$  value is not changing, so the values of  $C_r$  associated with the  $V/r$  cutoffs do not change. In Tests 1a and 1b, the input value of  $C_0$  is changing, and therefore the  $C_r$  value at which a given  $V/r$  threshold occurs changes too.

## 2.2 Results of the $C_0$ Sensitivity Computations

As noted in the previous section, the errors in derived visibility (due to  $C_0$  uncertainty) go to 0 when the target range equals visibility. At shorter ranges, the error can become quite large. Thus, all four of the plots show quite clearly that it is important to know the  $C_0$  value reasonably well. For example, from Test 1a, if the actual inherent contrast is .8, and if one wishes to have an error less than 20%, the error in  $C_0$  must be about .1 or less (when  $C_0$  is .8).

It is also quite obvious that the uncertainty is much less for ideal black targets than for non-ideal targets. In Test 1b, with actual inherent contrast of .5, the error can exceed 20% even if the contrast is known to within an uncertainty of .1 or less. This implies that if a non-ideal target is used, there will be loss of accuracy unless the  $C_0$  is very tightly specified, or the range of acceptable  $C_r$  values is more tightly limited.

Even if we accurately specify the  $C_0$  value at some point in time, the system is somewhat vulnerable to natural changes in  $C_0$ . As shown in Test 1c, the resulting visibility errors are probably reasonable when a target near  $C_0=.8$  is used. The error resulting from a change in  $C_0$  for targets near  $C_0=.5$ , shown in Test 1d, are quite large, implying that we probably should not use targets with  $C_0$  values as low as .5.

Even though these  $C_0$  sensitivity plots demonstrate a basic limit of system accuracy, there are some available trade-offs. We can help optimize system accuracy by utilizing a combination of several options such as:

- a) Limiting our targets to  $C_0$  values closer to 1; i.e. we should probably exclude any targets with  $C_0 < .5$ .
- b) Using  $V/r$  thresholds which depend on  $C_0$ . That is, we could allow  $V/r$  values as high as 4 when  $C_0$  is close to .8, but use a  $V/r$  limit which is smaller when  $C_0$  is less.
- c) Determine more accurate  $C_0$  values, and better characterize variations in  $C_0$  due to changes in horizon brightness, thus minimizing errors in input  $C_0$  as discussed below.

Study of the normally occurring  $C_0$  variations in the available targets of opportunity, in conjunction with the use of the plots (1a-1d) which show the impact of these variations, should allow us to optimize these tradeoffs.

Regarding option "c" above, there has been considerable interest in extracting the  $C_0$  values, as discussed in Section 5 of Johnson, et al, 1990. If the visibility for a given scene can be determined, either based on a median value for the targets, or based on an independent source, one should be able to back out the value of  $C_0$  required for a given target to yield that visibility value.

The first goal of a  $C_0$  study would be determination of the differing  $C_0$  values for a variety of targets. A second goal would be characterizing the variation in  $C_0$  over time for each target. This variation of  $C_0$  over time, for a given target, is caused by changes in  $iL_0$  as well as changes in  $pL_0$ . The changes in  $pL_0$  are most strongly driven by changes in scattering angle with respect to the sun; this should be well behaved. Changes in  $pL_0$  due to aerosol load should be more difficult to handle. Likewise, changes in  $iL_0$  due to the changing lighting distribution on the target, as weighted by the directional reflectance of the target, are complex. Whereas it should be possible to improve our current handling of input  $C_0$  values, we do not expect to fully predict the  $C_0$  behavior.

In order to enable a  $C_0$  study, it is first important to understand other sources of error on visibility; this was part of the reason for making this current study. It may also be important to derive curves, similar to those shown in the following section, which show the sensitivity of the extracted  $C_0$  value to various types of error. In this way, the study can be designed to maximize the  $C_0$  information returned, and minimize the impacts of measurement error on the  $C_0$  determination.



### 3.0 SENSITIVITY TO MEASURED TARGET UNCERTAINTIES

In any measurement system, there are limits to measurement accuracy. In the HSI, these can be caused by a number of factors such as measurement noise or non-uniformity in the basic chip sensitivity. This section discusses the impact of uncertainties in the measured target relative radiance.

#### 3.1 Computation of Sensitivity to Measured Target Uncertainties

The signal from the target is actually a relative radiance, in the sense that relative, but not absolute, radiances are determined over the scene. This is a result of the use of the auto-iris. The auto-iris causes a fixed percentage change over the whole scene. From the definition of apparent contrast, Eq. 2.3, it may be shown that these relative radiances yield an absolute measurement of apparent contrast.

The radiances are digitized on the image board by an A/D converter, to yield signals between 0 and 255. In this section we determine the error in computed visibility if there are known errors in this digitized signal. Signal noise is normally about 2-3 counts, whether the signal is near 0 or near 255. Many other types of signal errors we observe appear to be primarily additive, i.e. of a fixed value rather than a fixed percentage of the signal. Therefore, it was decided to determine the visibility error for signal errors of a given magnitude rather than a given percent. Errors of  $\pm 2$  and  $\pm 4$  counts, on the 0-255 scale, were selected.

An error in the measured target relative radiance will cause an error in the apparent contrast of the target with respect to the horizon sky. The resulting error in derived visibility is itself a function of the apparent contrast. In order to present the data in a manner which would be useful for further engineering studies, it was decided to plot the resulting error as a function of the measured apparent contrast, rather than the actual apparent contrast (because the HSI can only return the measured apparent contrast).

If there is an error given by the variable Err, the measured apparent contrast becomes

$$C_r = - \frac{({}_tL_r + Err - {}_bL_r)}{{}_bL_r} \quad 3.1$$

(where the minus sign converts to the positive  $C_r$  values used in the plots). Suppose one obtains a measured contrast of  $C_r$ , which includes an error as given in Eq. 3.1. One can show that the actual apparent contrast  $C_r'$  is related to this measured apparent contrast by

$$C_r' = \frac{{}_bL_r C_r + Err}{{}_bL_r} \quad 3.2$$

Then we can compute the visibility the HSI would return from using Eq. 2.2 with an input value of  $C_r$ , and we can compute the correct visibility (associated with 0 error) by using Eq. 2.2 with an input value of  $C_r'$ , as given by Eq. 3.2.

Note that by using this approach, in conjunction with Eq. 3.2, one derives the visibility error as a function of the measured (erroneous)  $C_r$  value. This is somewhat more complex than computing the visibility error as a function of actual apparent contrast (i.e. the

value that would have been measured in the absence of error). It was decided to use the measured apparent contrast in the plot, since this is the parameter which is available on the HSI.

As an example, if  $C_0$  is .8, and the measured horizon brightness is 100, as in Test 2a, and a measured  $C_T$  value of -.2 is obtained for a target at range 10 miles, this means that the measured target radiance was 80. If this target radiance measurement included an error of +4, then the actual target radiance should have been 76. That is, the measurement was +4 too high. Then the actual  $C_T$  value should have been -.24. The actual visibility, obtained from using .24 in Eq 2.2, is 23.0 miles, whereas the visibility returned by the HSI would be 20 miles, which is 13% low.

Tests 2a through 2d are plotted as a function of the measured  $C_T$ . Since Eq. 3.2 depends on horizon brightness, plots have been created for horizon brightnesses of 200, which are the normal setting, and 100, which is normally the lower limit. The results are also dependent on  $C_0$ , and have been computed with  $C_0$  values of .8 and .5.

### 3.2 Evaluation of Sensitivity to Measured Target Uncertainties

The deviations in the Test 2 series are somewhat less, in general, than those shown in the Test 1 series. That is, the sensitivity to measured target uncertainty is in general less than the sensitivity to  $C_0$  uncertainty. The error in visibility is most sensitive to measured target uncertainties at low  $C_T$  values, i.e. when the target range is close to the visibility. That is, whereas the 4.0 V/r cutoff is critical in minimizing errors due to  $C_0$  uncertainties, it is the other end, the 1.15 V/r cutoff, which is critical in minimizing errors due to  $C_T$  uncertainties.

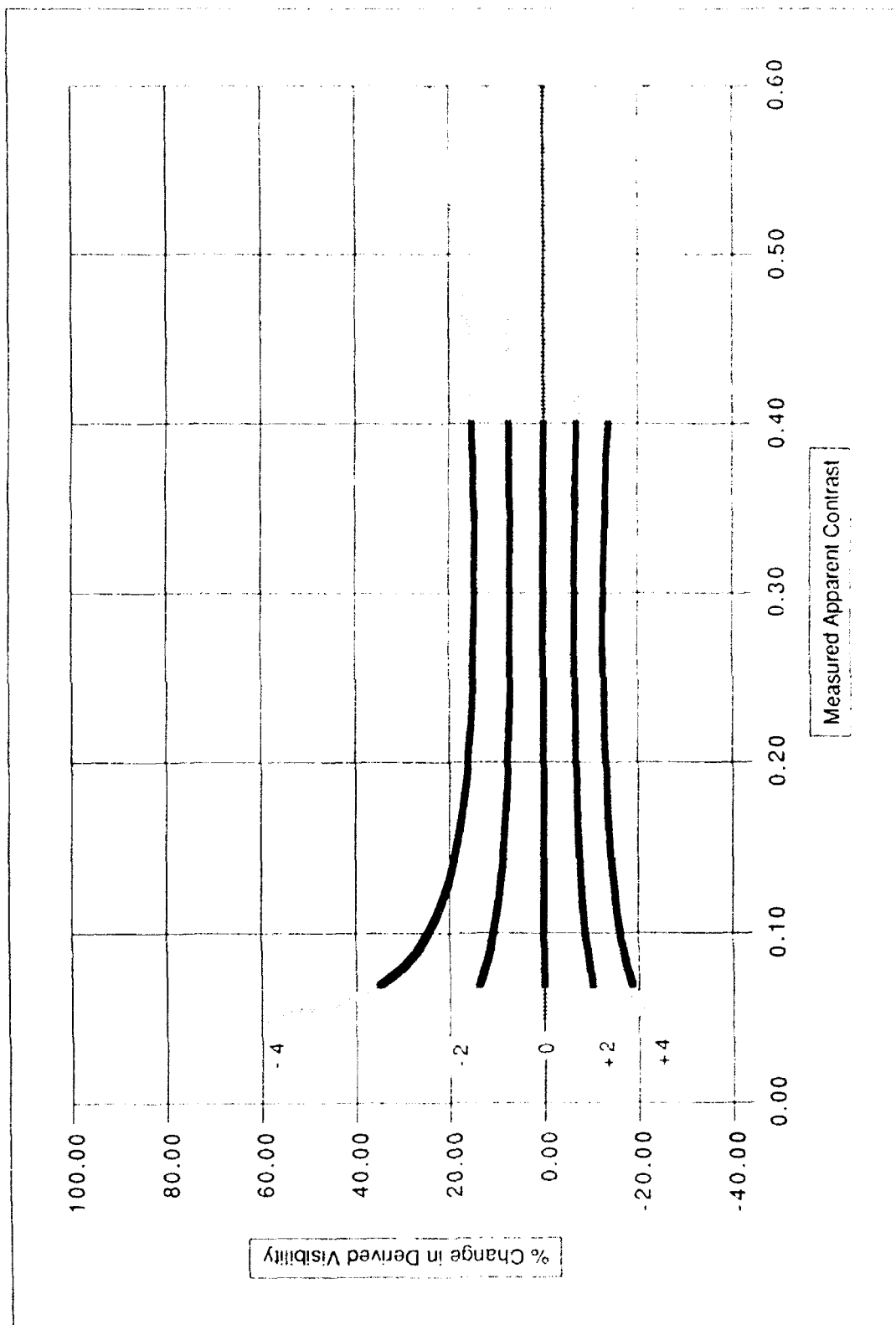
A comparison of Tests 2a and 2b shows immediately that there is considerable advantage, in terms of this type of error, in keeping the horizon radiance high. If the auto-iris is set so that the horizon radiance stays near 200, and targets with  $C_0$  near .8 are chosen (Test 2b), the error resulting from a measurement error of  $\pm 2$  is less than 5% over most of the span.

The situation is not quite so good when targets with  $C_0$  values near .5 are chosen, as shown in Tests 2c and 2d. Test 2c illustrates that the combination of low  $C_0$  and low horizon radiance are the worst case. In this plot, the error resulting from a measurement error of  $\pm 2$  is between 10 and 20%.

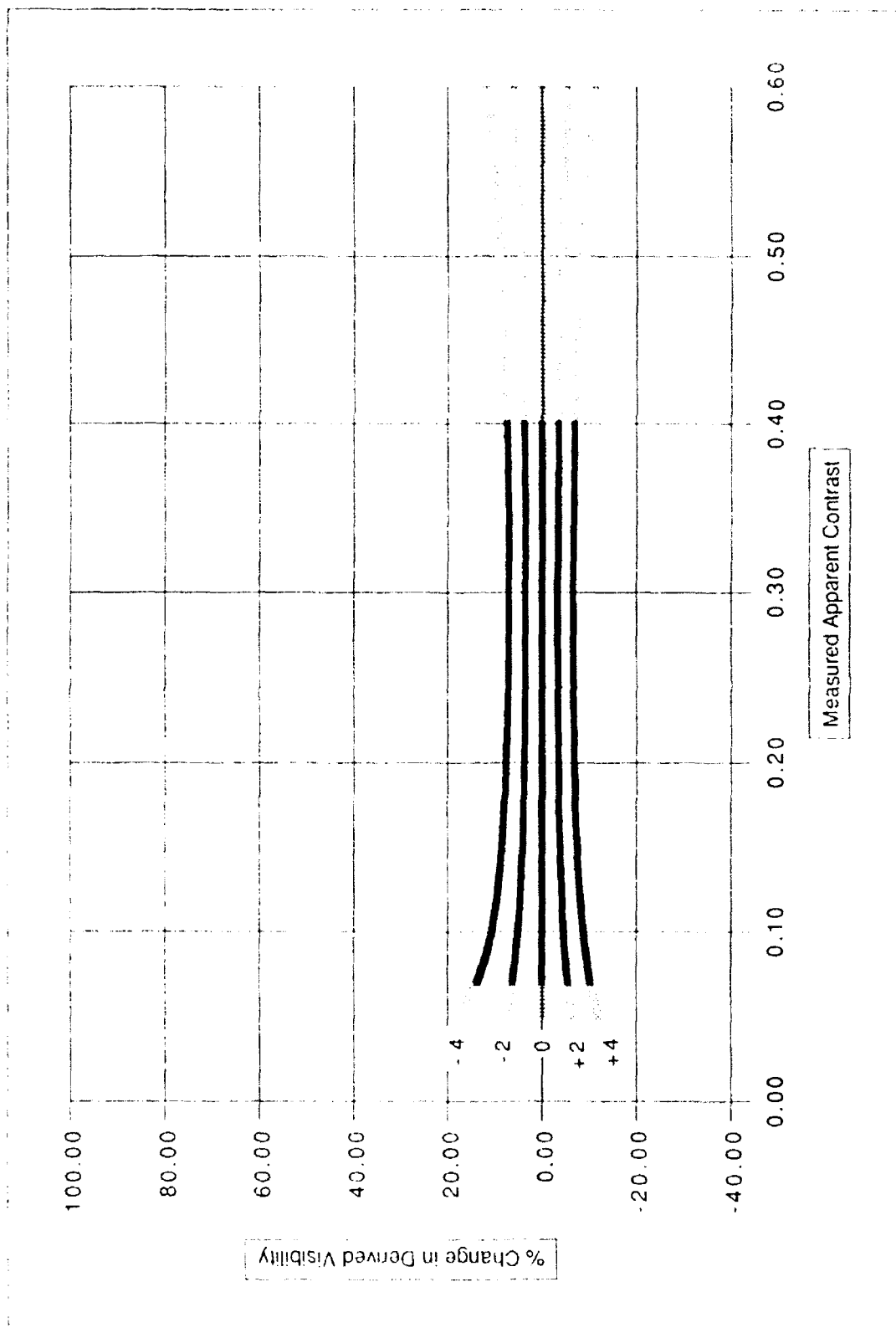
An obvious first step in utilizing these results is to ensure that the auto-iris is set so that the measured horizon radiances are reasonably high, i.e. near 200.

It would be useful to determine the source and magnitude of typical measurement errors. Whereas the electronic noise can create an error of 2-3 counts in a specific pixel, the measured target radiances are normally the average of several pixels, and should not be subject to large random errors. We need to determine the typical error due to noise in the spatially averaged signal. If it is too large, additional temporal averaging could be used to minimize it.

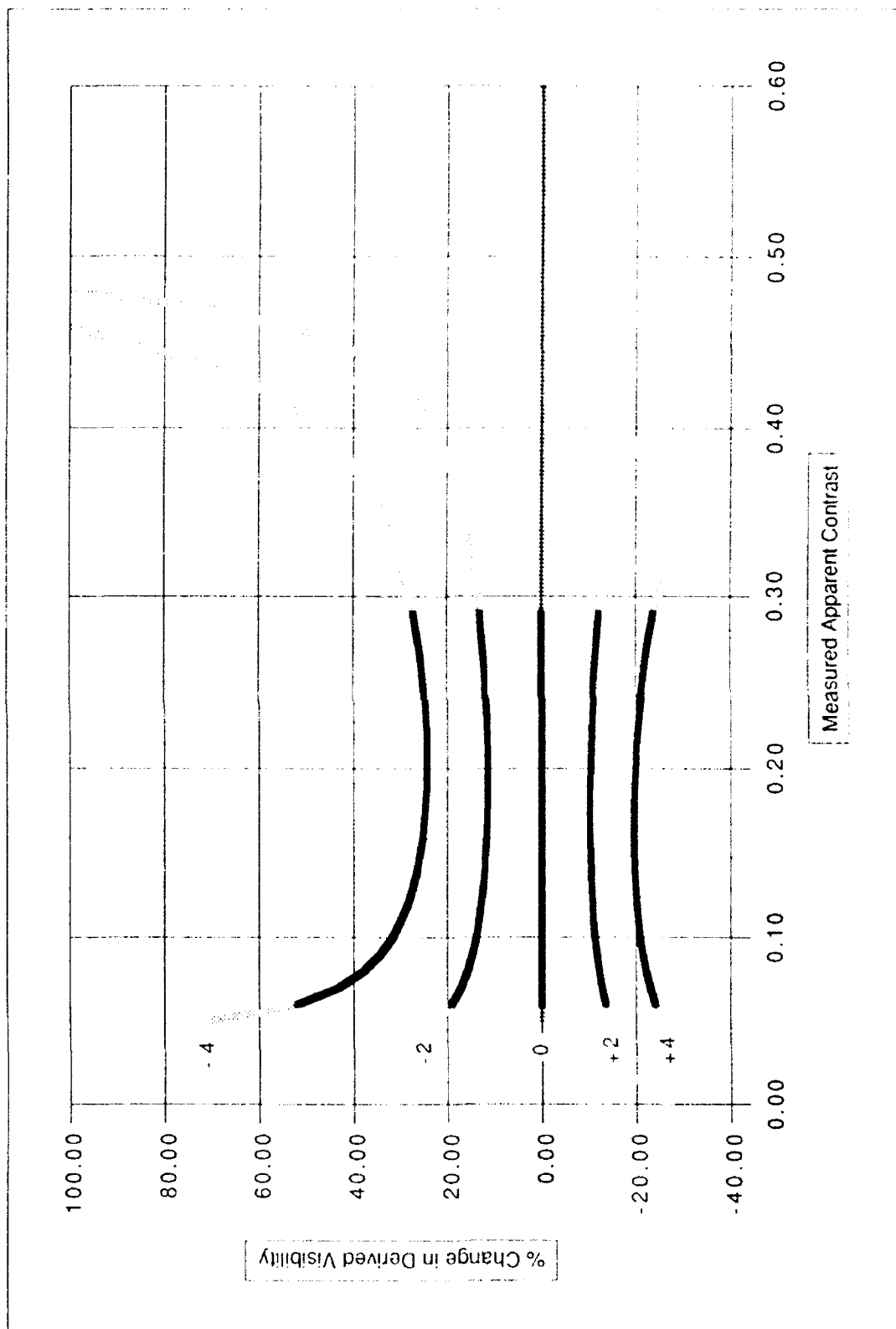
A slow rise in the dark current signal could also contribute to a measurement error. This may be more important than the noise, since spatial averaging does not decrease the error. Again, the data needs to be evaluated to determine typical error magnitudes. If necessary, a light trap could be installed at one azimuthal look angle, to enable measurement and correction of the dark signal.



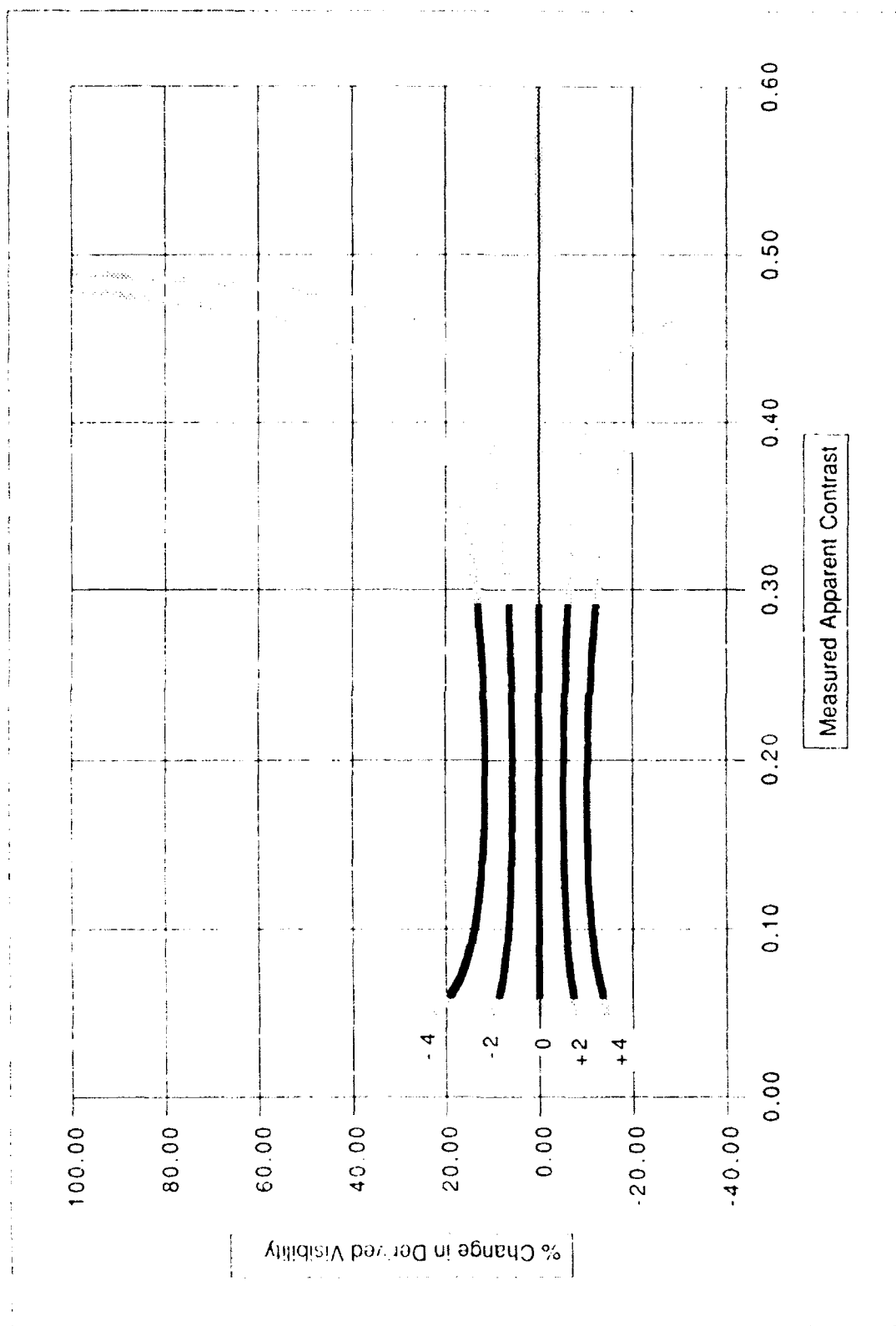
Test 2a Sensitivity of Derived Visibility to Measured Target Radiance Uncertainty  $Co = 8$   $Lq = 100$



**Test 2b** Sensitivity of Derived Visibility to Measured Target Radiance Uncertainty Co = 8 Lq = 200



**Test2c** Sensitivity of Derived Visibility to Measured Target Radiance Uncertainty Co = 5 Lq = 100



**Test 2d** Sensitivity of Derived Visibility to Measured Target Radiance Uncertainty  $C_0 = 5$   $Lq = 200$

Another source of measurement error is the spatial non uniformity in the sensor chip. This can be evaluated by extracting the signal for the various target positions, from a calibration measurement taken with uniform lighting on the chip. (This calibration measurement has already been acquired at a variety of light levels, as part of the linearity calibration.) If this non-uniformity is found to be large enough to cause a significant error (as indicated by Tests 2a-2d), the non-uniformity could easily be compensated for in the visibility algorithm.

As with the  $C_0$  sensitivity study, the plots which have been generated show the sensitivity of visibility to a given error; in this case a measurement error. It remains to determine the magnitude of the measurement errors which exist, and then decide which if any of the above correction procedures seem warranted.

#### 4.0 SENSITIVITY TO MEASURED HORIZON BRIGHTNESS UNCERTAINTIES

Just as there may be errors in the determination of the target relative radiance, there may be errors in the determination of the horizon relative radiance. These errors fall into two quite distinct categories. There may be measurement errors, in which the returned signal is incorrect due to noise, dark current, or chip non-uniformity. And there may be errors in the visibility determination because the measured background sky is not in fact the same as the equilibrium radiance, due to either misplacement of the horizon region of interest, or contamination of the region of interest by clouds, or other obstructions to visibility.

In either case, there is an error in the determination of what is assumed to be equilibrium radiance. If this error has a given magnitude, in terms of signal change, the net effect on the derived visibility will be the same. Thus, although these plots are primarily intended to show the effect of measurement error, they can also be used to evaluate the impact of deviations from the ideal clear horizon. Test set 3a-3d evaluates the sensitivity of derived visibility to the measurement uncertainties.

##### 4.1 Computation of Sensitivity to Measured Horizon Uncertainties

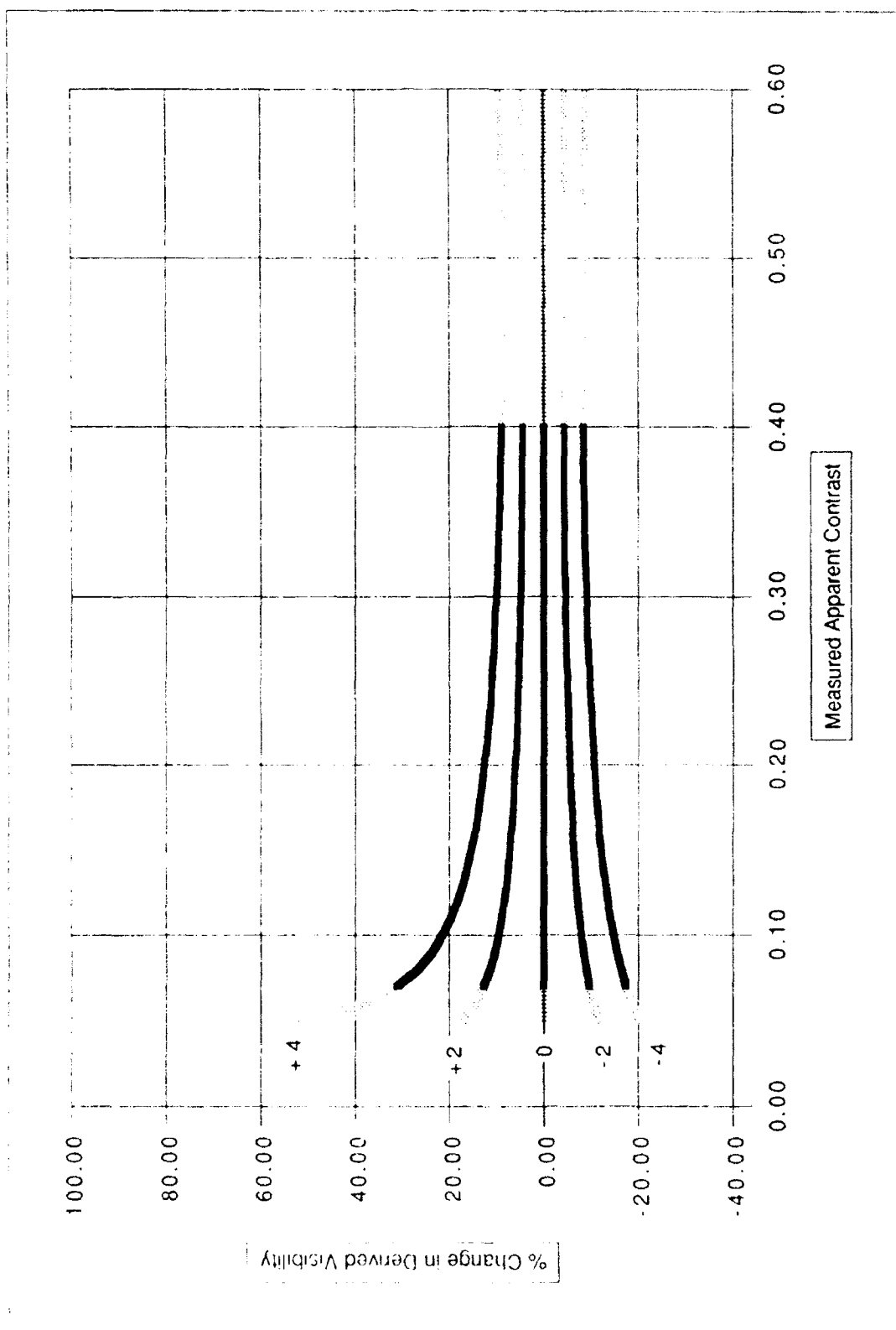
As with the earlier plots, we wish to plot the errors as a function of the measured (rather than actual) apparent contrast. If there is a measurement error in the horizon radiance, then the measured apparent contrast (allowing for the change in sign) becomes

$$C_r = \frac{-(I_r - ({}_h I_r + Err))}{{}_h I_r + Err} \quad 4.1$$

(similar to Eq. 3.1). Then it can also be shown that for a measured  $C_r$  value, as given above, the correct value of apparent contrast,  $C_r'$ , is given by

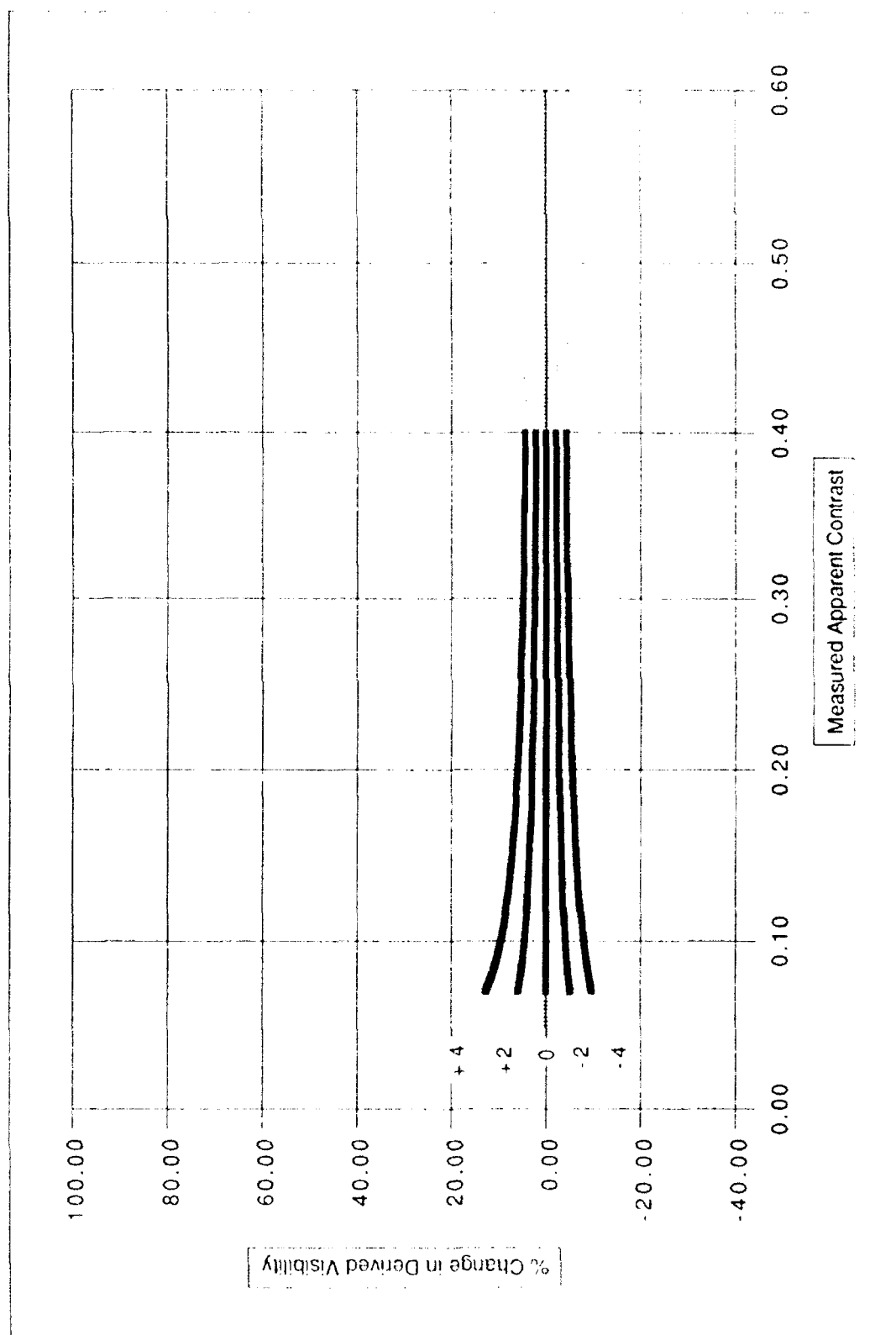
$$C_r' = \frac{C_r {}_h I_r + Err(C_r - 1)}{{}_h I_r} \quad 4.2$$

Since this is similar in concept to the derivation of the error resulting from target measurement uncertainty, I will not show a numeric example. As with the previous test set, sample computations have been made for horizon radiances of 100 and 200, and  $C_0$  values of .8 and .5.

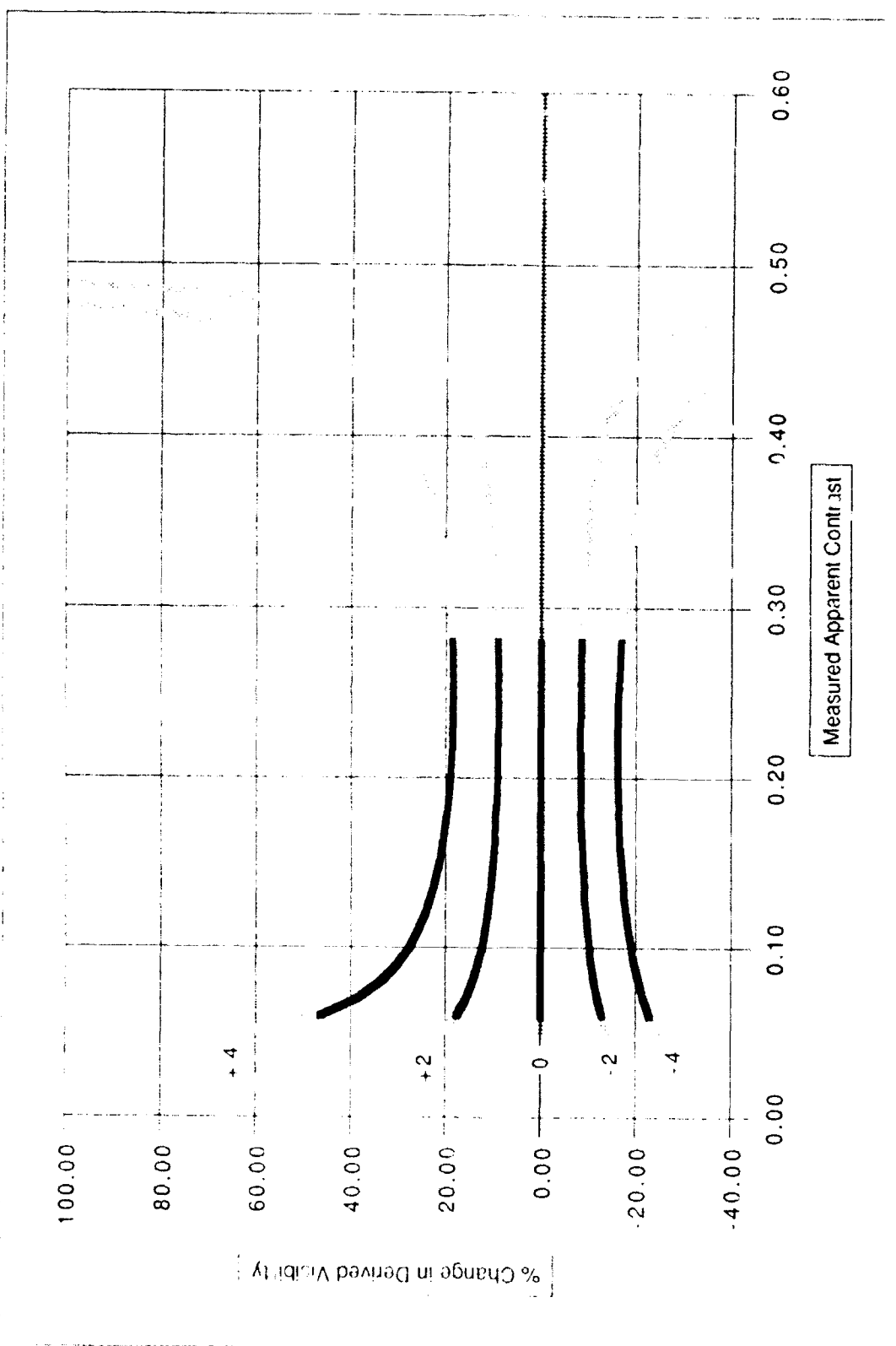


**Test 3a** Sensitivity of Derived Visibility to Measured Horizon Radiance Uncertainty  $C_o = .8$   $L_q = 100$

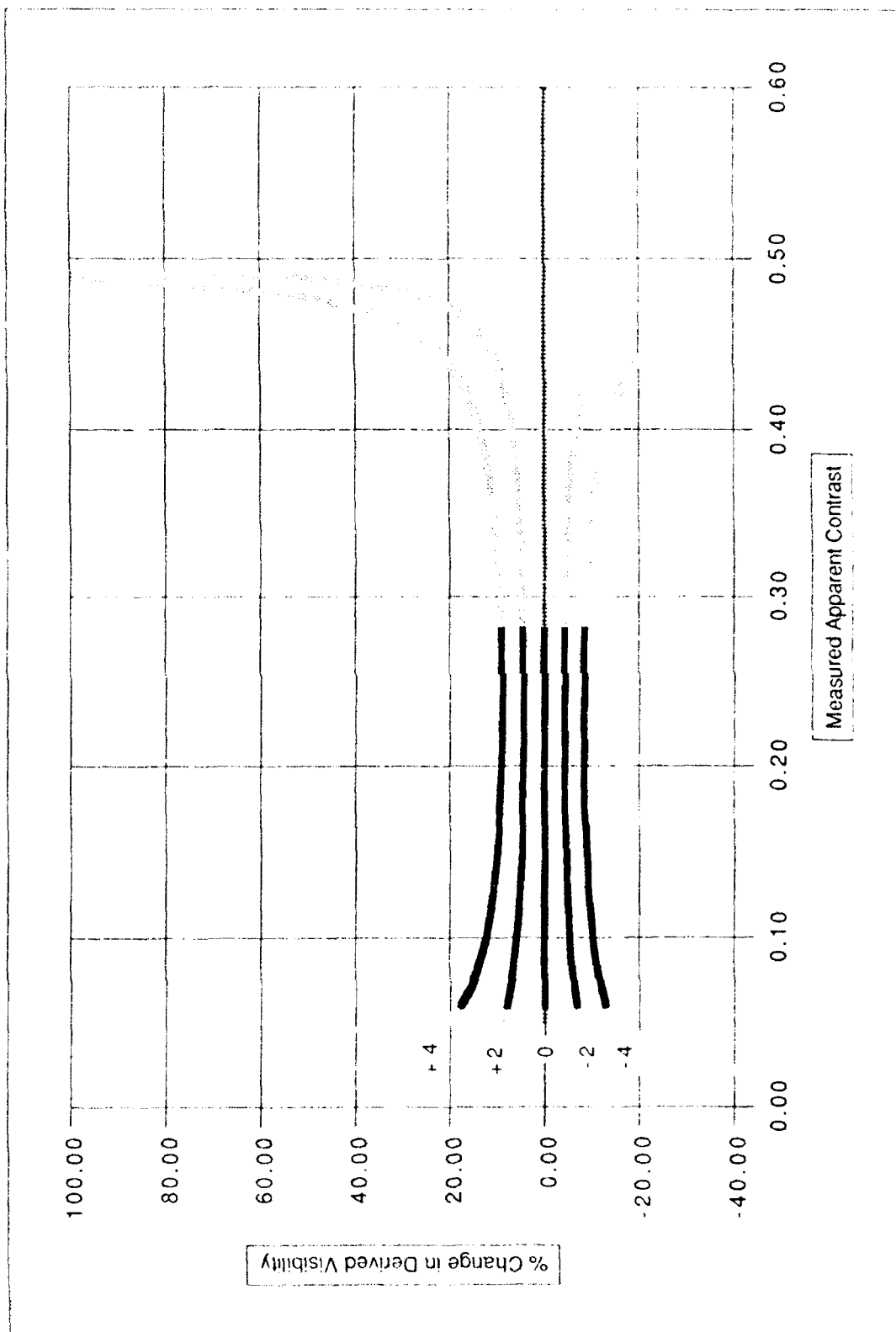




**Test 3b** Sensitivity of Derived Visibility to Measured Horizon Radiance Uncertainty Co = 8 Lq = 200



**Test 3c** Sensitivity of Derived Visibility to Measured Horizon Radiance Uncertainty  $C_0 = .5$   $Lq = 100$



**Test 3d** Sensitivity of Derived Visibility to Measured Horizon Radiance Uncertainty  $C_o = 5$   $Lq = 200$

## 4.2 Evaluation of Sensitivity to Measured Horizon Uncertainties

Plots 3a-3d are quite similar to plots 2a-2d. On each of the four plots, the largest error occurs when  $C_T$  values are near .05. That is, as with Plots 2a-2d, the worst effect of the measurement error occurs when the target range is close to the visibility. The V/r cutoff at 1.15 protects the system from the largest errors (in the grey region of each line).

A comparison of plots 3a and 3b (as well as 3c vs 3d) shows the significant advantage in keeping the horizon radiance values near 200 (through proper setting of the auto-iris). Similarly, a comparison of plots 3a vs 3c, and 3b vs 3d, shows the advantage of using dark targets, with inherent radiances close to .8 (or close to 1, ideally).

As with the previous tests, follow-up action should include evaluation of the magnitude of typical errors. The horizon radiance can be impacted by the same measurement errors mentioned in Section 3.2, namely noise, dark offset, and chip non-uniformity. In addition, we need to evaluate the magnitude of the signal error due to misplacement of the horizon region of interest (ROI) or corruption of the scene by clouds. It might be reasonable to acquire two horizon ROI's, and evaluate the standard deviation in each ROI as well as the comparative brightness. In this way the HSI could automatically detect cases in which the horizon is impacted by clouds. Evaluation of the data to determine the merit of these various schemes for improving equilibrium radiance determination seems appropriate.

## 5.0 SENSITIVITY TO NON-LINEARITY OF CAMERA RESPONSE

The CID sensor chips in the camera, in conjunction with the camera electronics, yield a reasonably linear camera response. That is, the output signal is in general proportional to the input brightness (or relative radiance in object space). However, the relation is not perfect, particularly near the high end of the camera sensitivity range. Therefore an evaluation of sensitivity to this type of error seems appropriate.

### 5.1 Computation of Sensitivity to Measured Non-linearity

Computations of the error resulting from camera non-linearity are relatively straight forward. Linearity calibrations have been acquired for all cameras; they are reduced as discussed in Memo AV89-056t. The output of a linearity calculation is a look-up table. For each measured signal value, this table lists a corrected signal which is linearly related to the original radiance generating the measured signal.

If the horizon has a measured brightness given by  $hI_T$ , and the measured contrast is  $C_T$ , it can be shown that the measured target radiance is given by

$$hI_T = hI_T (1 - C_T) \quad 5.1$$

(allowing for the change in sign in  $C_T$ ).

For a given  $C_T$  value, the visibility returned by the HSI is given by Eq. 2.2. The visibility which has been corrected for the non-linearity may be obtained by running the horizon radiance through the linearity look up table, running the target radiance in Eq. 5.1 through the look-up table, and recomputing visibility.

As an example, let  $C_0$  equal .8, and the horizon radiance equal 100, as in Test 4a. When  $C_T = .2$ , the  $hI_T$  value computed from Eq. 5.1 is 80. Application of the linearity table

for the first system (linearity test LIN020) corrects the value of 80 to 82.2, and the value of 100 to 100.7. The corrected contrast, derived from Eq. 2.3, becomes .184. The corrected visibility, from Eq. 2.2, is then 18.8 when the target range is 10. The visibility returned by the HSI can be directly computed from Eq. 2.2, using  $C_T = .2$ ; this value is 20, which is thus about 6% high.

As in the previous sections, these computations have been run for  $C_0 = .5$  and  $.8$ , and horizon radiance = 100 and 200. In addition, computations have been made for horizon radiance = 220, for the following reasons. The camera sensitivity tends for most systems to be reasonably linear over most of the span, but tends to become increasingly non-linear as the upper limit of 255 is approached. Since the error can become somewhat critically dependent on the horizon radiance above 200, it was decided to run additional calculations for a horizon signal of 220. The resulting set of 6 plots are labeled Test 4a through Test 4f.

In each plot, four curves are given. The first curve, from linearity LIN020, is for the camera which is currently at Otis. The third, LIN028, is for the camera currently at MPI. The other two are randomly chosen linearities (the ones that happened to be on my computer), and were acquired for cameras used in WSI units. They are included to give the reader a better feel for the range of values that might occur.

## 5.2 Evaluation of Sensitivity to Measured Non-linearity

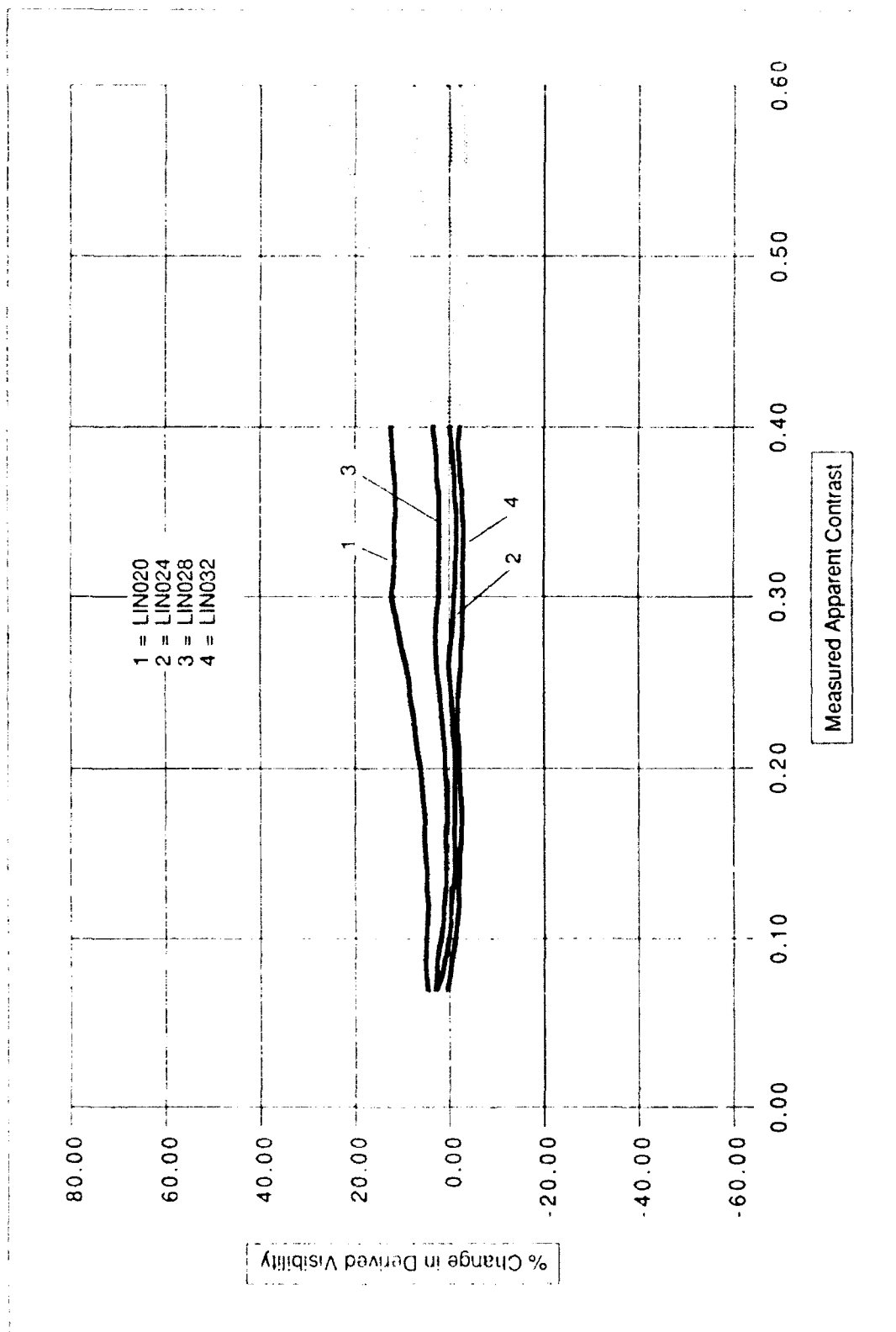
The sensitivity curves for the linearity are not so well behaved as the earlier plots. Consider first Tests 4a through 4c, i.e. those with  $C_0 = .8$ . In Test 4b, one can see that for  $L_q$  values of 200, all four cameras yield pretty similar results: the error is about -5% to -10%, and essentially independent of the  $C_T$  value. When the horizon radiance is higher, at a level of 220 (Test 4c), one of the cameras, represented by LIN024, has a quite large error of about 25%. This occurs because this one camera is still reasonably linear at a signal of 200, but is somewhat non-linear at the signal of 220. At the  $L_q$  value of 100, shown in Test 4a, three of the systems are quite accurate, but one is about 10% high.

The plots for  $C_0 = .5$ , Tests 4d through 4f, are similar in character, although the magnitudes of the errors become somewhat larger.

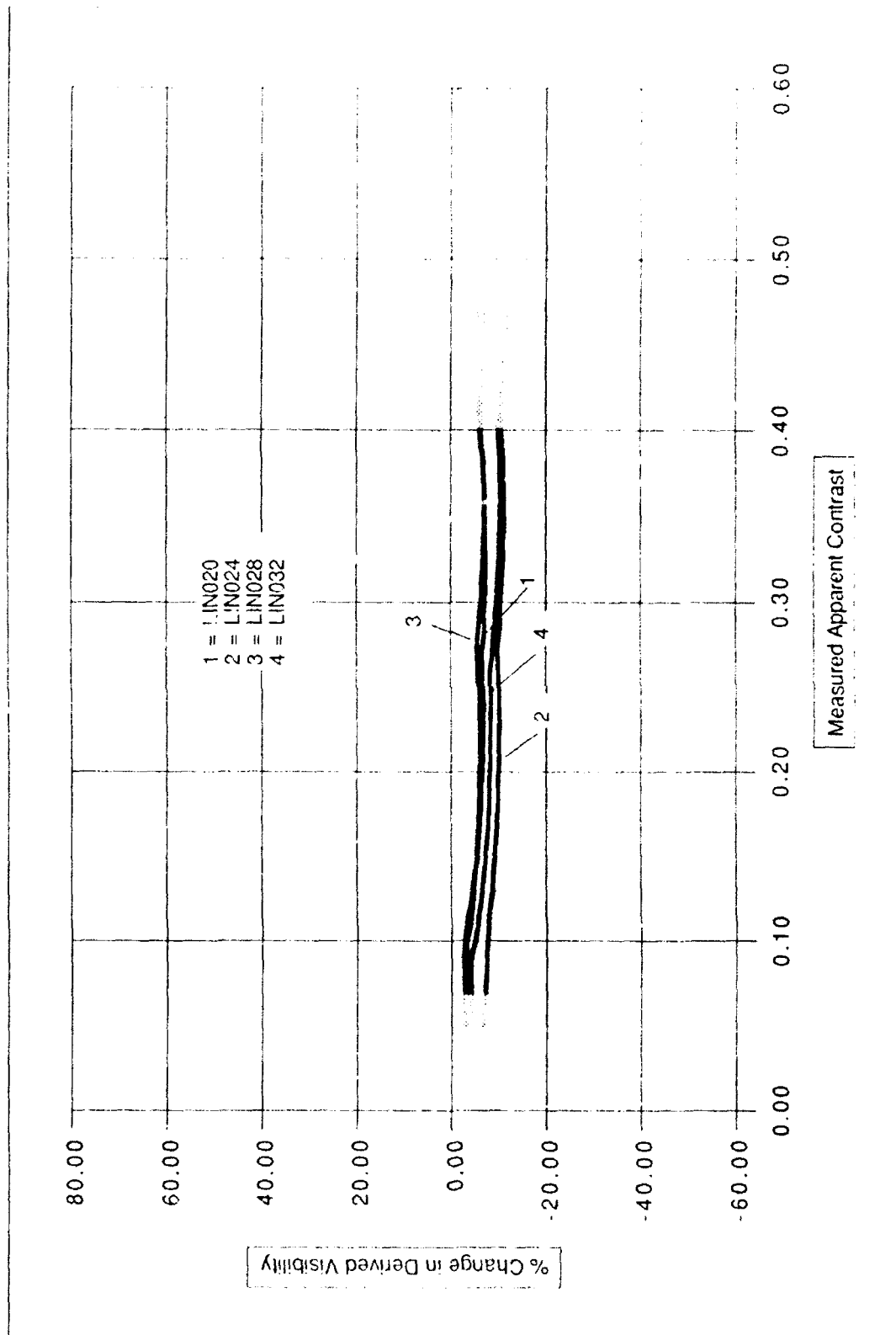
As noted above, several of the plots, such as Test 4b, show little variance in the percent error as  $C_T$  is varied. This implies that in a given scene, both near and far targets would have roughly the same percent error. Thus the non-linearity of the camera causes, in this example, an overall bias in the visibility determination, rather than a lack of consistency between the individual target returns.

It is helpful to understand why the effect of the non-linearity can be so large. Consider the case of the horizon radiance set at 200, and an inherent contrast of  $.8$ . The  $V/r$  limits serve to limit the  $C_T$  range to  $.07$  to  $.4$ . In terms of target radiance, this means that the signal can be used only if it is between 120 and 186. This means that only a somewhat narrow range of signals are being used in the visibility determination. The determination is essentially based on difference measurements; precision becomes quite critical. The numeric example in Section 5.1 is a good example of this. The linearity correction was only about 2.2 at a signal of 80 (a 3% correction), yet the impact was a 6% change in determined visibility.

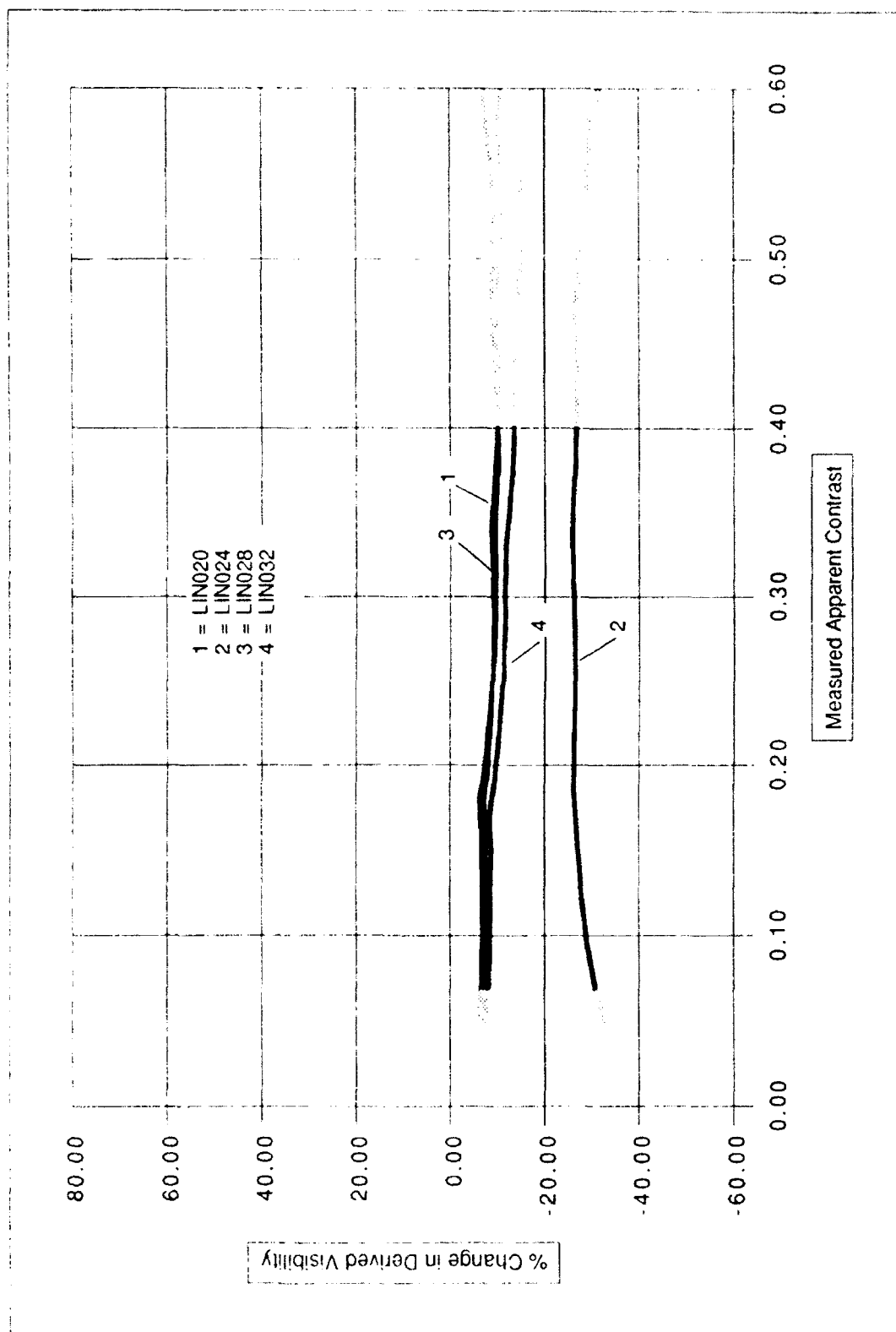
The non-linearity is an instrumentation characteristic which can be compensated for in the software. To the extent that we are able to characterize the system response accurately, and to the extent that that response does not change, we should be able to make reasonable



**Test 4a** Sensitivity of Derived Visibility to Non-Linearities in Camera Response Co = 8 Lq = 100

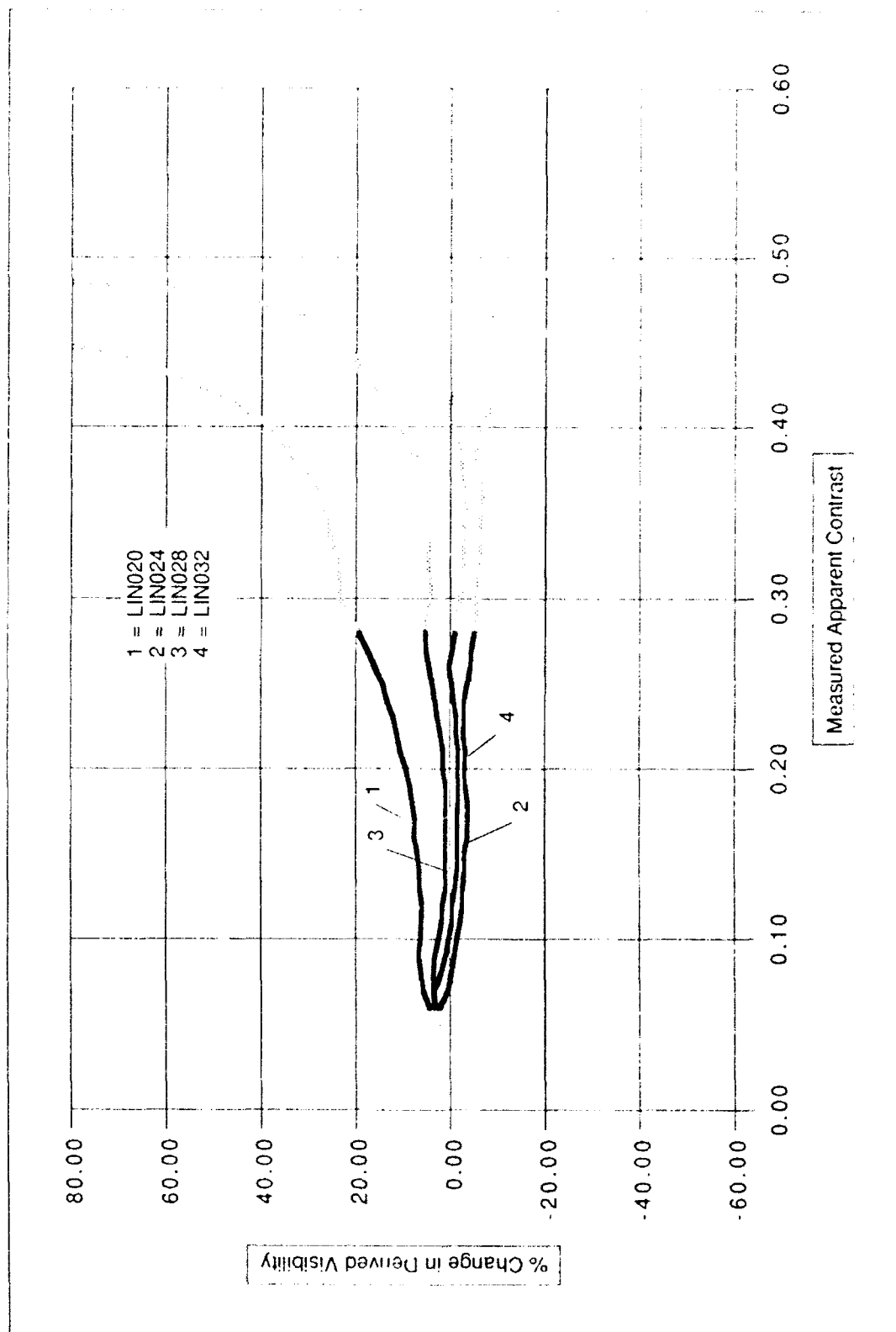


Test 4b Sensitivity of Derived Visibility to Non-Linearities in Camera Response Co = 8 l q = 200

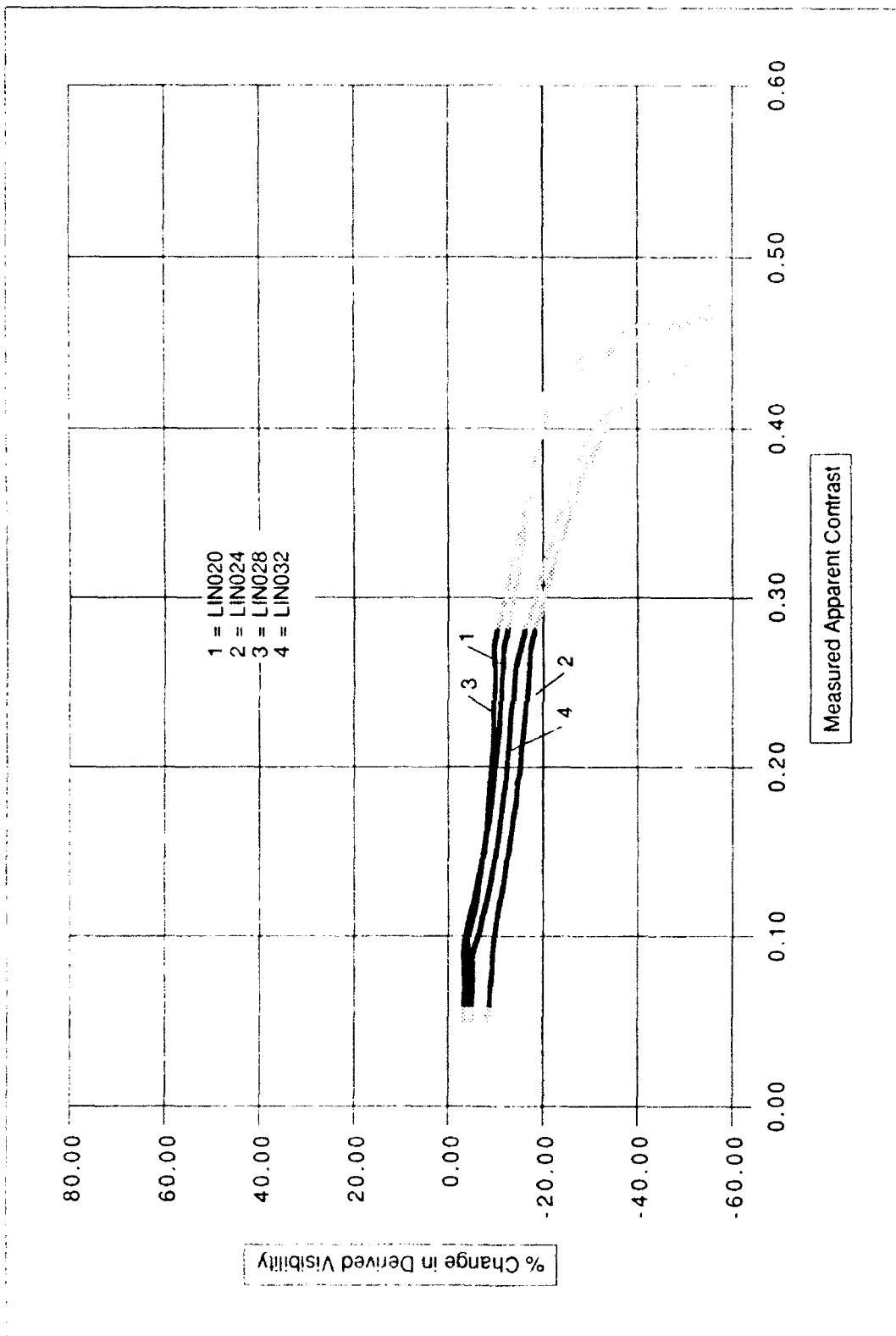


**Test 4c** Sensitivity of Derived Visibility to Non-Linearities in Camera Response Co = 8 Lq = 220

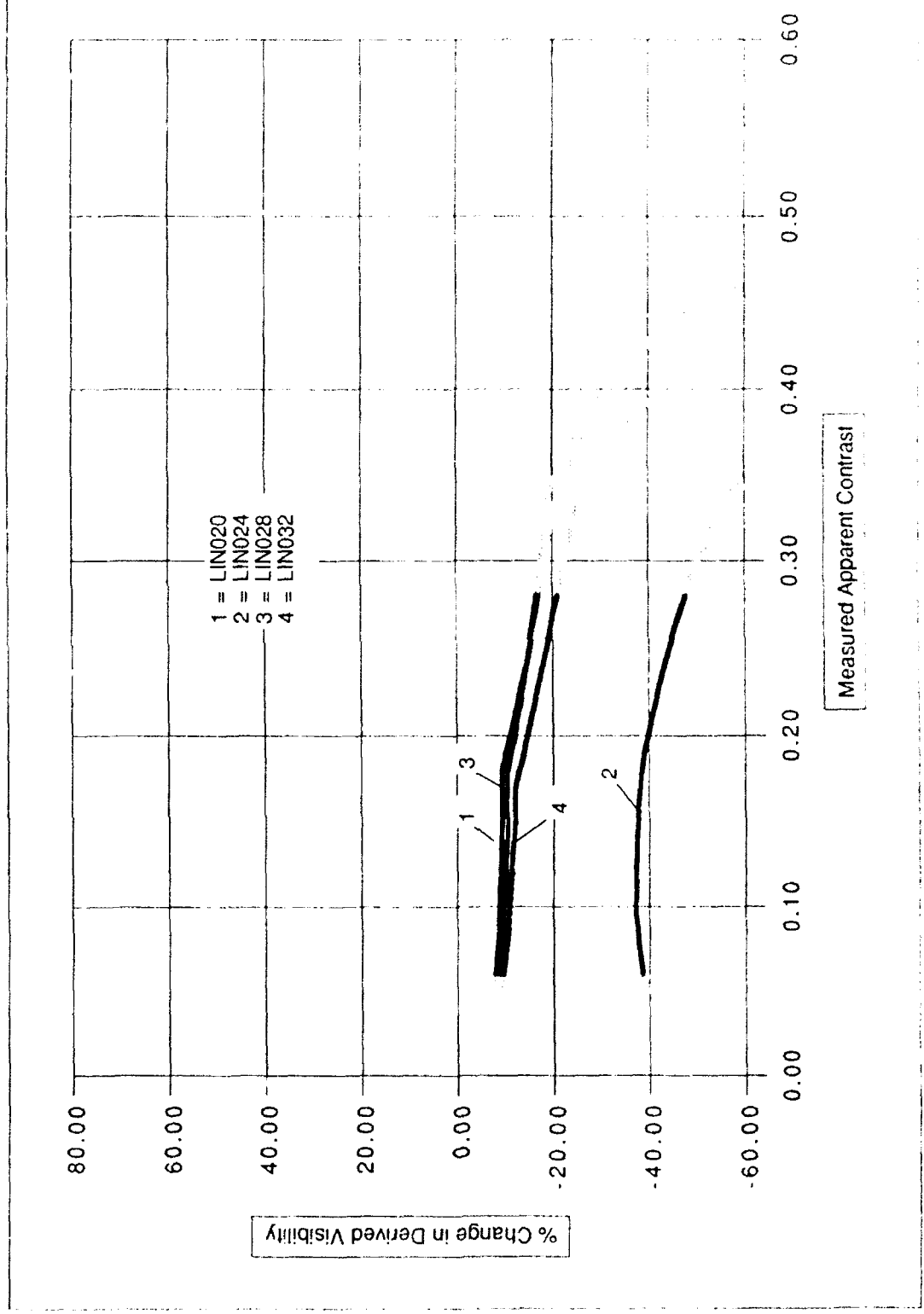




**Test 4d** Sensitivity of Derived Visibility to Non-Linearities in Camera Response Co = 5 l q = 100



**Test 4e** Sensitivity of Derived Visibility to Non-Linearities in Camera Response Co = 5 Lq = 200



Test 41 Sensitivity of Derived Visibility to Non-linearities in Camera Response Co = 5 Lq = 220

corrections. The next section discusses further the extent to which this system response can be characterized.

### **5.3 Characterization and Stability of System Response; Implications**

As noted above, the linearity correction can be quite critical. Applying a linearity correction is easy and quick, in terms of software development and processing time. However it is important that the application of the linearity actually represent an improvement. In order for this to be true, we must be able to measure the system response accurately, and the response must be reasonably stable.

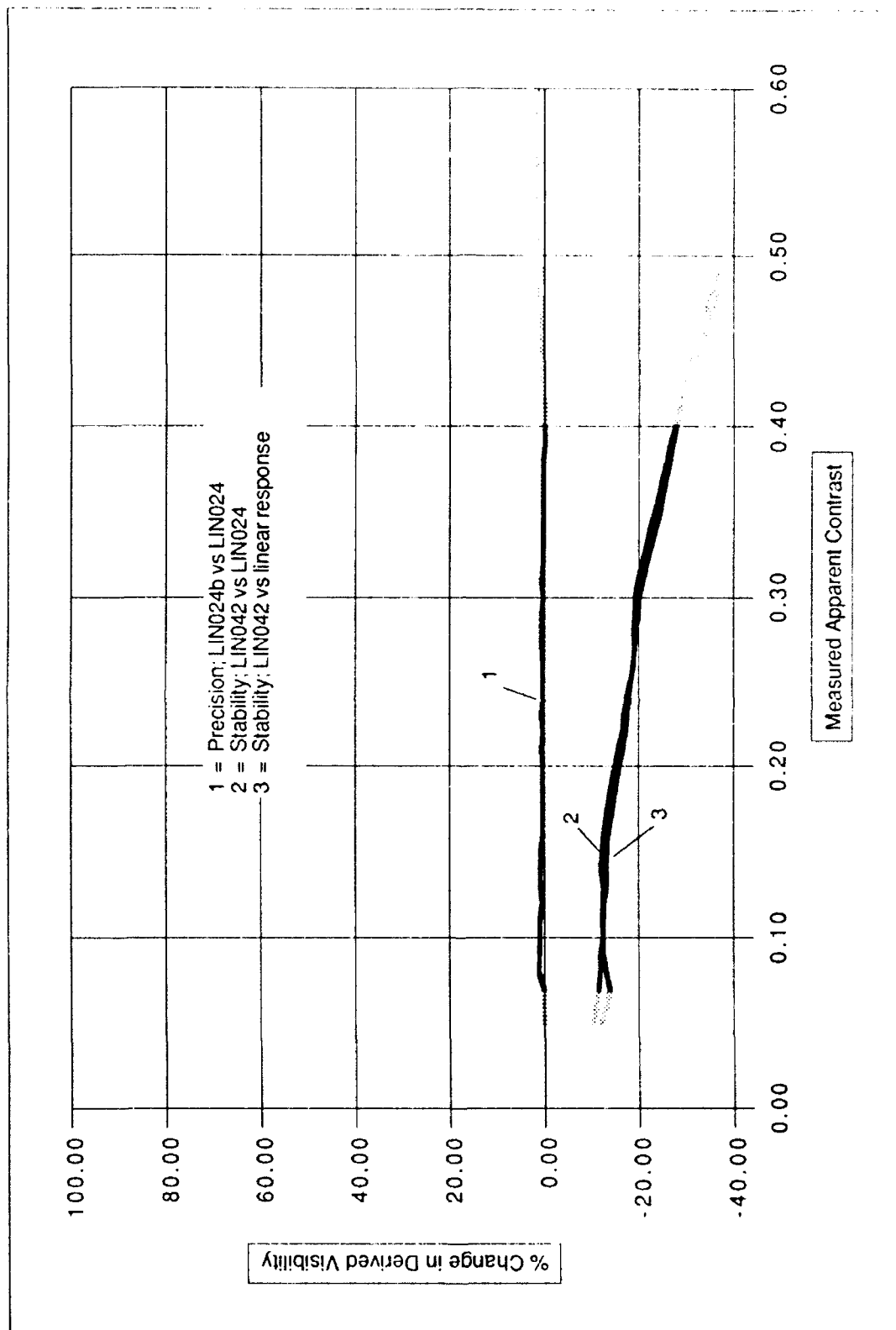
In order to evaluate the extent to which these two conditions of accuracy and stability are true, three more plots labels Test 5a through Test 5c were generated. It turns out that one of the systems characterized in the Test 4 series was fielded for over a year, and then returned for post calibration. This system, characterized by linearity LIN024, was chosen for study.

First, in order to characterize the measurement accuracy, a closer look at LIN024 was taken. During the linearity calibration, a duplicate set of measurements is acquired. First, the lamp is moved through a set of positions to characterize the change from the bright end to the dark end. Then a repeat set of data is acquired, moving this time from the dark end to the bright end. Suppose that at some point in time the repeat set of data on the linearity accurately characterize the system response, but we use the initial linearity data set to make our correction. The resulting error gives a measure of our measurement uncertainty caused by signal to noise ratio, in terms of its impact on the visibility determination. This is what is shown in Curve 1 of Plots 5a through 5c. The errors are quite small: nearly always less than 1%. Thus measurement error in the linearity determination is probably not enough to cause a problem. (Another test was run in which a camera was calibrated using two different calibration setup configurations, to characterize our measurement error caused by stray light or other setup errors. The impact of this difference on the visibility determination is less than 3%.)

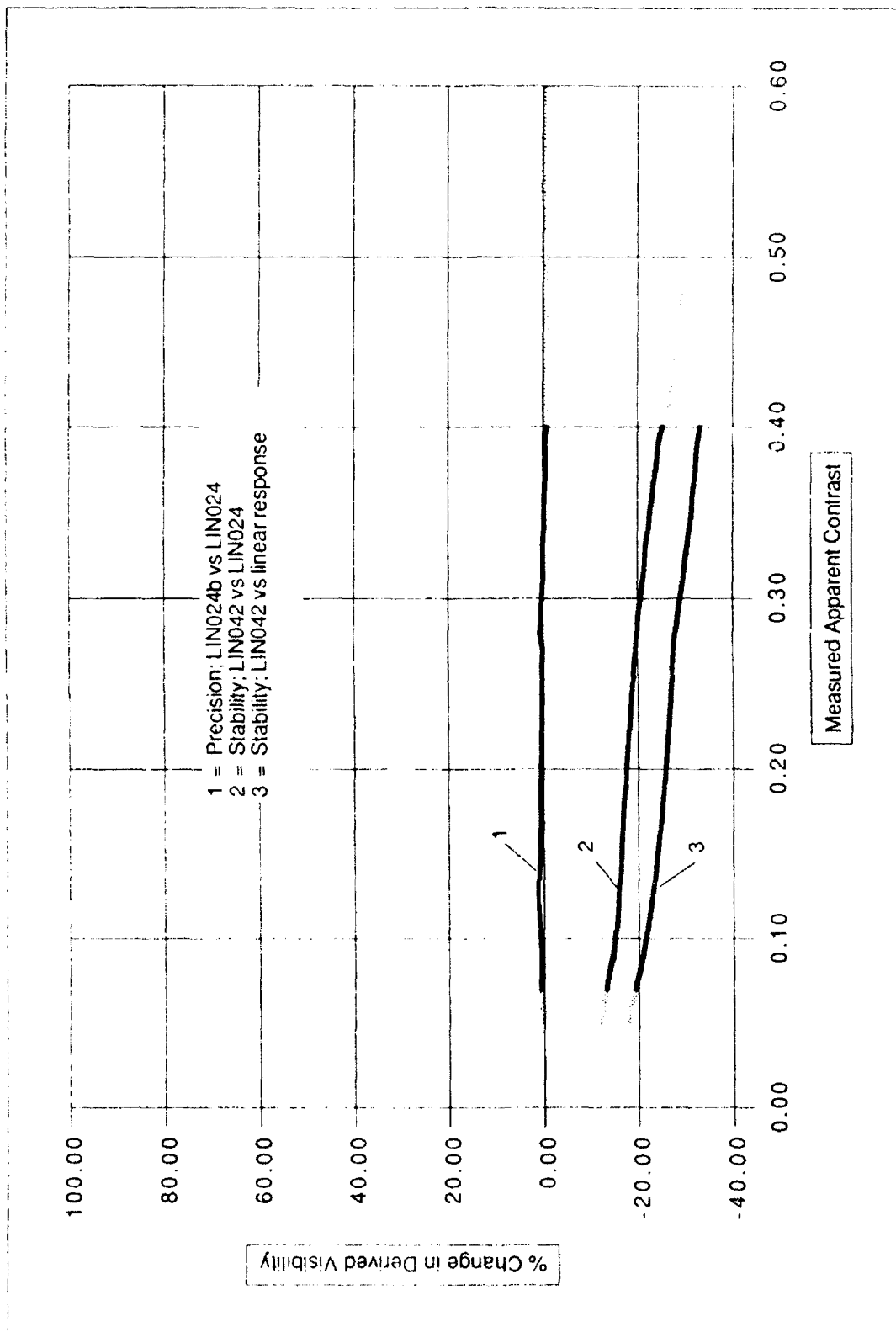
It is also important to test the impact of stability of system response. The camera calibrated in LIN024 was taken into the field (in a WSI unit) and run 24 hours a day for over a year. On return, it was recalibrated (LIN042), and found to be somewhat truncated. The full dark value had come up from a signal of 1 to a signal of 15, and the full bright value had decreased from 226 to 210. Thus both ends had contracted by counts of about 15. This is not unexpected after a year in the field.

Two curves have been computed from this linearity data. Curve 2 in Plots 5a through 5c, labeled 42 vs 24, shows the impact on the visibility if the camera actually has the response indicated by LIN042, but the user applies the linearity correction based on LIN024. Thus, if one had measured the camera response as shown in LIN024, and applied this consistently, but the camera drifted over time to the response indicated by LIN042, the resulting error in the computed visibility would be as shown in Curve 2. Curve 3 shows the error if the response is as indicated by LIN042, and no linearity correction is made. Thus these two curves show the impact of drift in system response, with and without the use of the pre-deployment calibration.

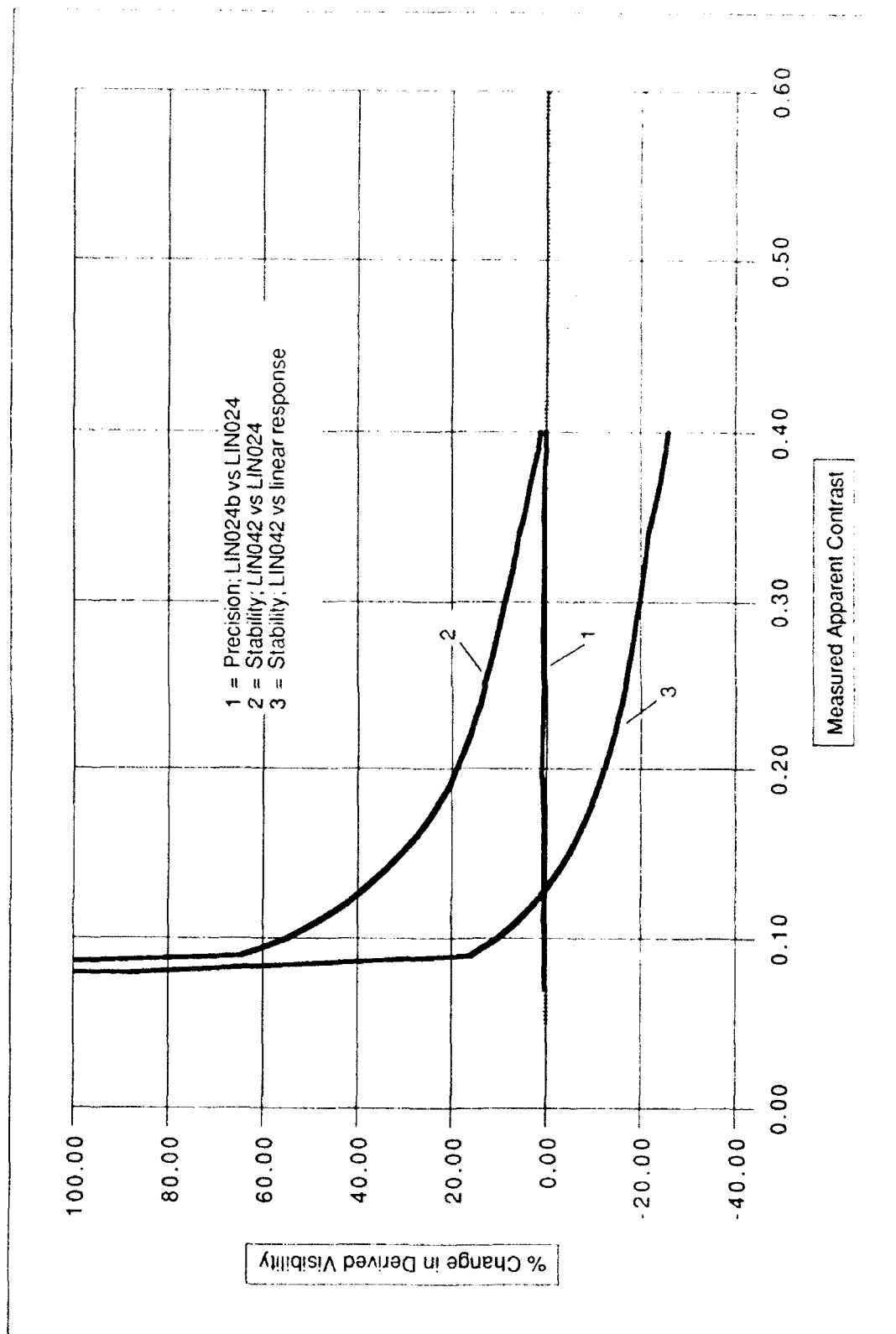
The error shown in curves 2 and 3 of Plots 5a through 5c is disconcertingly large. It is probably not atypical. Most of the cameras experience an increase in the dark level of 15 to 30 counts in the period of a year or more, and many experience high end truncation. The HSI unit may or may not have had a similar change. It has not been calibrated in 2 years, but it may not change as much per year due to its much shorter duty cycle of only a few



Test 5a Sensitivity of Derived Visibility to Precision and Stability of Non-Linearity Co = 8 Lq = 100



**Test 5b** Sensitivity of Derived Visibility to Precision and Stability of Non-Linearity Co = .8 Lq = 200



Test 5c Sensitivity of Derived Visibility to Precision and Stability of Non Linearity Co = 8 Lq = 220

hours a day. The fact remains that this is a very significant source of error that deserves some attention.

Over the short run, an immediate answer to the problem of drift in the system response is to recalibrate the sensors more frequently. In particular, we need to check the response of the two units currently in use in HSI units. Over the long run, the use of some sort of in-field calibration device may be warranted. Placing a light trap in the field of view at the home position should allow us to monitor the increase in the full dark level. The occasional use of an artificial source which would saturate the image (radiometrically) would allow monitoring of the high end truncation.

If feasible, the use of a field calibration device which could provide well defined relative flux levels within an image might allow *in-situ* determination of the effective response curve, for in-field updating of the linearity curve. In short, the type of error indicated by Test 5 is one that should be reasonably avoidable, through proper calibration of the camera, but it is an error that is apparently important to avoid.

## **6.0 SENSITIVITY TO TARGET RANGE AND CONTRAST THRESHOLD**

In the previous sections, plots have been shown which illustrate the system sensitivity to errors in the input  $C_0$  value, errors in the measured target and horizon radiances, and errors due to system response non-linearity. There are two remaining input values: the target range, and the  $\epsilon$  threshold.

### **6.1 Sensitivity to Target Range**

In considering errors in target range, it is probably reasonable to consider the fractional error. For a target which is near, it is reasonably easy to pinpoint its location within a small radius. For a farther target, it is increasingly difficult to pinpoint its location: the expected uncertainty might be a given fraction of the target distance.

The sensitivity of visibility to errors in target range of a given percent is quite easy to compute. From Eq. 2.2, it may be shown that an error of  $x\%$  in range yields an error of the same percent in visibility. That is, if one inputs a range value which is  $5\%$  high, the resulting visibility will be  $5\%$  high. This is a simple enough relationship that no plots were made. It is safe to conclude that if the HSI is to be accurate within a given percent, the target ranges must be accurate to that percent.

### **6.2 Sensitivity to Contrast Threshold**

The situation with visual threshold  $\epsilon$  is somewhat different. It is my opinion that this number should not normally be varied. Visibility is defined in terms of a threshold contrast of .05. The human has a threshold contrast of approximately .05, if the target size and light adaptation level are maintained, along with other parameters such as glimpse time.

The human threshold contrast is significantly changed if these conditions are changed. For example, if the human looks at a very small target (or very large), the threshold contrast will change, and the human will make an erroneous determination of visibility. If we choose to change the input  $\epsilon$  value in the HSI, we can simulate the human error, and estimate the expected error that the human might make. In general however, the HSI should try to return the correct visibility, not what the human might call with an inadequate target. We do this by maintaining the input  $\epsilon$  value associated with the definition of



visibility. Therefore for this sensitivity study, it was not deemed appropriate to determine sensitivity to changes in  $\epsilon$ .

## 7.0 SUMMARY

Two summary plots, containing curves extracted from the earlier sections, have been created: one for  $C_0 = .8$ ,  $L_q = 200$ , and one for  $C_0 = .5$ ,  $L_q = 200$ . In these plots, the four curves show: the impact of a  $C_0$  change of .1; the impact of a measured target radiance change of 4 (on the 0 to 255 scale); the impact of a measured horizon radiance change of 4; and the impact of system non-linearity for the system at Otis.

All of these uncertainties can cause a certain amount of error. The sensitivity to  $C_0$  uncertainty is very small when the target range is close to the visibility (near  $C_T = .05$ ), and fairly large when the target is closer. Unfortunately however, the measurement uncertainties cause the most error when the target range is close to the visibility. That is, when the  $C_0$  impacts are least, the measurement error impacts are largest.

There are some techniques for improving our  $C_0$  estimates, but in the final analysis the  $C_0$  changes may be most difficult to handle. The measurement uncertainties may in many cases be mitigated by a combination of improved measurements techniques and improved data reduction techniques. As the magnitude and/or impact of measurement uncertainties are improved, it should be possible to chose targets closer to the visual threshold, which should help mitigate the impact of the  $C_0$  uncertainties.

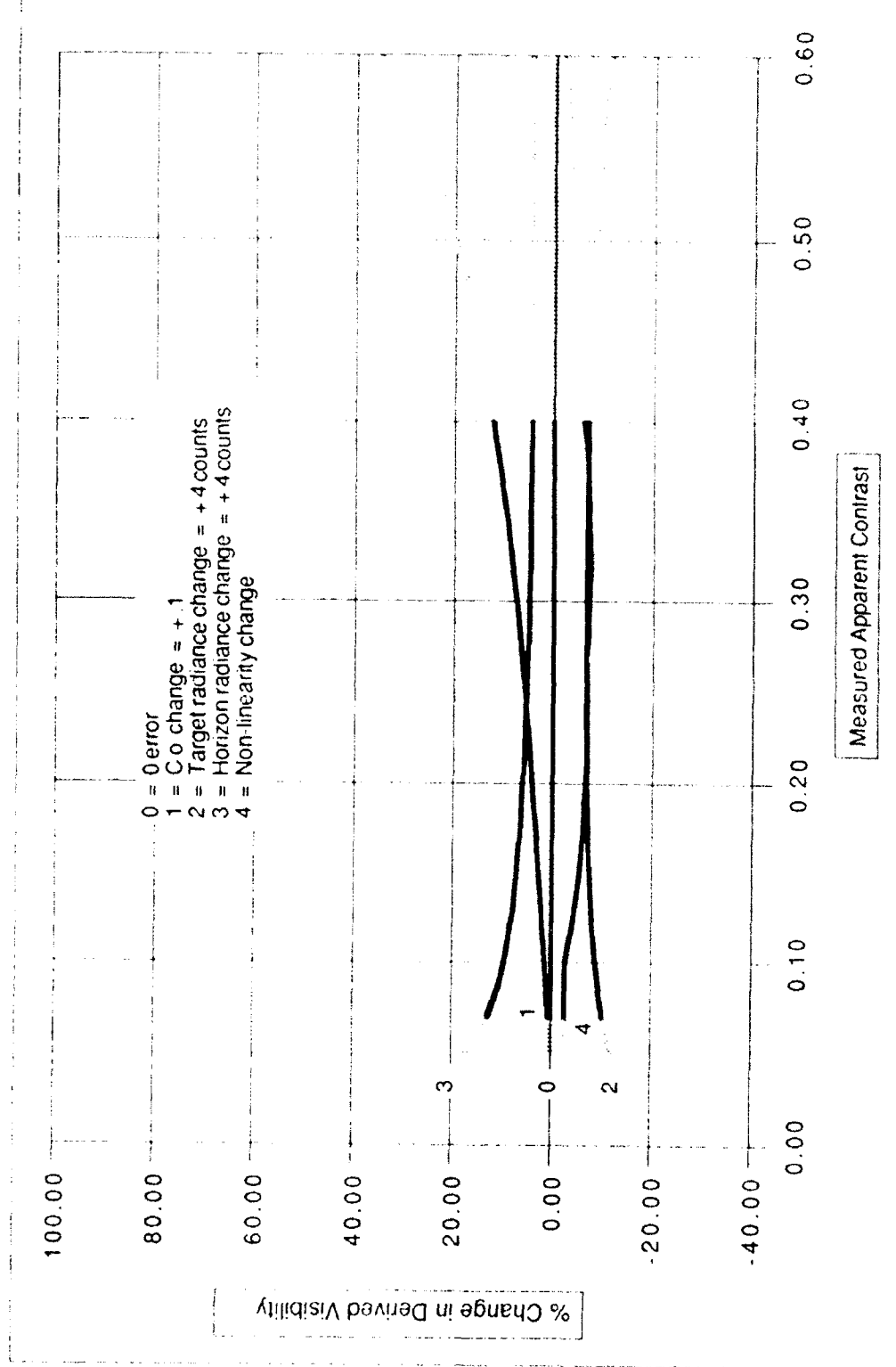
Another way to look at the system is to consider that the ability to determine visibility from targets ranging near the visibility depends on the ability to accurately determine the difference between signals which are quite close. This requires precision, stability, and accuracy in the measurements acquired by the system. At the other extreme, the ability to determine visibility from targets which are at close range (and which therefore have apparent contrast somewhat close to the inherent contrast) depends on our ability to accurately characterize the  $C_0$  values and their fluctuations.

In the short run, there are obvious ways in which improvements can be made in terms of measurements. These include keeping the horizon radiance near 200, and measuring and applying the non-linearity correction. Other potential improvements such as correcting for chip non-uniformity, to improve measurement accuracy, may or may not be warranted. There are a variety of tests to help us determine questions such as this one.

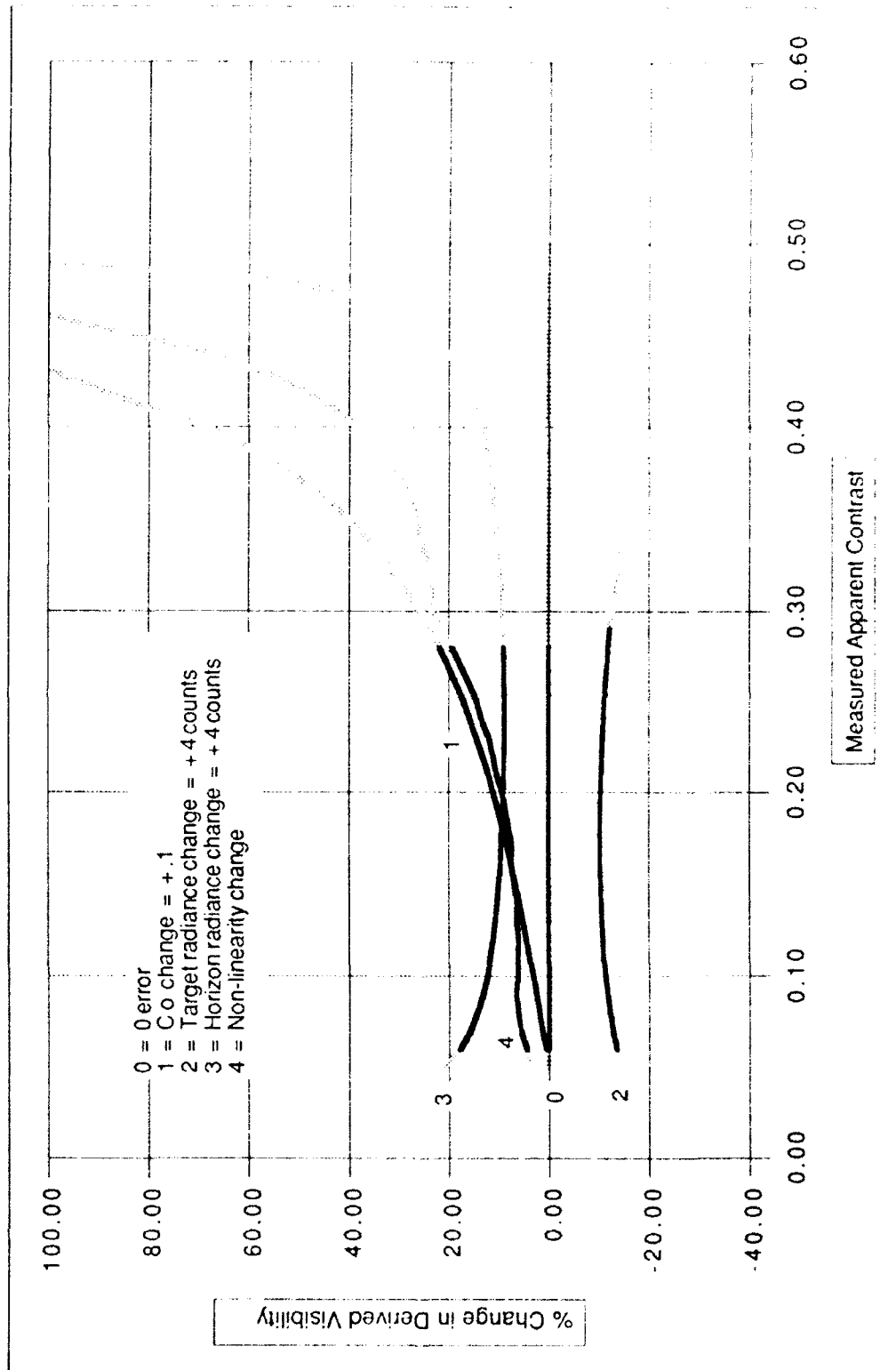
A significant improvement in the current accuracy should be readily realized as these changes are enacted. In the long run, as solid state sensors improve in stability and noise handling, we should expect significant improvements in the measurement capabilities. These in turn should allow us to make better use of the measurement regimes in which the sensitivity to  $C_0$  changes becomes small.

## 8.0 RECOMMENDATIONS

As an outcome of this study, there are a number of changes and/or tests which should be considered. These fall roughly into two categories. The first category is changes having to do with measurement accuracy, including both improvements to the measurement accuracy, and changes to mitigate the impact of measurement inaccuracy. The second category is changes having to do with the handling of non-ideal measurement conditions, such as non-ideal targets or non-ideal horizon skies. These two types of improvement categories will be discussed below.



Summary a for Co = .8 Lq = 200



Summary b for C<sub>0</sub> = .5 Lq = 200

## 8.1 Improvements Relating to Measurement Accuracy

The first and most obvious change I would recommend is to ensure that the horizon radiance is near 200 counts. Whereas this does not in itself increase the measurement accuracy, it significantly mitigates the effects of measurement inaccuracy. With the MPL unit, the horizon signal is currently near 100; we need to verify that the camera response has not become truncated due to internal problems, and then adjust the auto-iris to yield a horizon brightness near 200. With the Otis unit, we similarly need to determine the current signals which occur for the horizon, and optimize them as necessary.

We need to acquire a new linearity calibration for the MPL unit, to determine how much change, if any, has occurred since the original calibration. It will be somewhat more difficult to acquire a linearity calibration for the Otis unit, but this is certainly something to do when possible. I would propose that we incorporate application of the linearity correction into a test version of the software. We should devise a technique for testing the sensor response in the field. Installation of a light trap, to enable testing of the dark end of the responsivity curve, could help us begin testing the efficacy of this sort of *in-situ* procedure.

Next, there are several tests that involve investigation of the magnitude of existing measurement errors. As discussed earlier, both the horizon and target radiances are impacted by noise, changes in full dark, and chip non-uniformity. Any change in full dark may be treated as part of the sensor responsivity change documented by the linearity calibration, and need not be treated separately for now.

The magnitude of system noise averaged over the horizon and target ROI's may be evaluated by grabbing several images of the same scene in close temporal succession, and comparing the resulting signals averaged over the ROI's. The errors due to chip non-uniformity may be evaluated using the linearity calibration data. If one wants to know the magnitude of non-uniformity for a given target location, one extracts the signal for that target ROI and for the horizon ROI, but using a calibration image of a uniform source. We can then decide if either system noise or chip non-uniformity cause errors large enough to require compensation.

Since the impact of measurement error is worst as  $V/r$  approaches the lower limit of 1.15, and the impact of non-ideal  $C_0$  is worst as  $V/r$  approaches 4.0, there is benefit in avoiding these limits. Since the optimum range is a function of the visibility, it is important to have enough targets so that there are always several within the optimum range, for all possible visibility values.

Within the limits imposed by the availability of real world targets, an effort should be made to select many targets over a range of target distances. (For those familiar with transmissometers, it may be helpful to note that whereas a transmissometer is reasonably accurate over a range of visibility values determined by its base length, the HSI is reasonably accurate over a range of visibility values determined by the target ranges. By using very near targets under low visibility conditions, and far targets under high visibility conditions, we are creating an impact similar to adjusting the transmissometer base length.)

Note also that it is very important that the range to these targets be determined accurately, since the error in visibility due to an error in range is directly proportional to the range error. This may involve driving out to the sites, and visually identifying the targets being used.

## 8.2 Improvements Relating to Non-ideal Conditions

There are several things which can be done to improve the system with regard to non-ideal conditions. First, consider the impact of horizon sky problems. If the measured horizon radiance is not equal to the equilibrium radiance, there is a corresponding error in the visibility. Under clear sky conditions, the near-horizon radiance is expected to decrease away from the equilibrium radiance value as the elevation angle is increased. This occurs due to the decreasing turbidity of the path of sight.

It would be instructive to extract the change in horizon radiance over the range of elevation angle in the HSI field-of-view. This can be done with existing HSI imagery. This would allow us to determine the range of elevation angles which provide a sufficiently accurate determination of the equilibrium radiance (in the absence of clouds).

Similarly, we should investigate the incidence of clouds on the horizon which are bright enough to cause error. We can probably improve our handling of this possibility by using two horizon ROI's, and checking the signal standard deviation in each, as well as the difference in the average signals. If one ROI has a high STD and/or elevated signal, use of the other ROI might avoid the cloud. If both ROI's have high STD's, there is probably little that can be done currently other than alert the user, or potentially not use the visibility for that scene. A test program to investigate these possibilities should be implemented.

Over the longer run, the case of cloud clutter at the horizon might be addressed by the next generation larger field-of-view WSI. If we make determinations using the WSI of where the clouds are, it should be feasible to utilize horizon ROI's which are in the clear areas indicated by the WSI. Similarly, introduction of a red/blue filter changer to the HSI could allow determination of the clear horizon regions for use in visibility determination.

Finally comes the really difficult problem, changes in  $C_0$ . Once we have improved the accuracy of the system in the ways discussed above, we will probably want to tackle determination of  $C_0$ . This is done by using the median visibility determined from the available targets, or an independently determined visibility, then determining what  $C_0$  values for each target will yield that visibility.

It would be very helpful to run curves similar to the ones in this technical note which determine the sensitivity of the  $C_0$  determination to known errors, so that we can adjust our technique appropriately. (For example, we know intuitively that the targets must be at close range, relative to the visibility, in order for visibility to be sensitive to  $C_0$ , which means targets must be close to back out the  $C_0$  value. But does measurement error then cause undue problems?)

If we are successful with  $C_0$  extraction, a study of the time variation in  $C_0$  would be helpful. The equilibrium radiance is expected to change as a function of the scattering angle with respect to the sun. This gives us a theoretical change in  $C_0$  due to the change in the horizon brightness. If this is dominant over changes due to target brightness, the diurnal changes in  $C_0$  might be reasonably predictable.

## 9.0 CONCLUSION

This note has presented plots illustrating the sensitivity of the visibility derived from the HSI measurements to a variety of sources of uncertainty. In general, the errors depend on the magnitude of the apparent contrast, which in turn depends on the relative values of visibility and target range. The sensitivity to measurement error is maximized when the

target range is close to the visibility; the sensitivity to inherent contrast, on the other hand, is greatest when the target range is much less than the visibility.

This study has defined some obvious ways to improve the system, as well as some areas requiring investigation of the data. Over the long term, retrofitting the HSI with the new generation of cooled solid state sensors provides potential for further improvement. With less noise, higher radiance resolution, and better stability, these cameras should allow more precise measurements and a corresponding improvement in the visibility determinations from the HSI.

## 10.0 ACKNOWLEDGEMENTS

The authors would like to recognize the outstanding work of Carole Robb, publications support at Marine Physical Laboratory, in preparation of the plots and text.

## 11.0 REFERENCES

- Douglas, C. A., and R. L. Booker (1977), *Visual Range: Concepts, Instrumental Determination, and Aviation Applications*, U. S. Department of Transportation, Federal Aviation Administration, Systems Research and Development Service, Report No. FAA-RD-77-8, Washington, D. C. 20590.
- Duntley, S. Q., A. R. Boileau, and R. W. Preisendorfer (1957), *Image Transmission by the Troposphere I*, University of California, San Diego, Scripps Institution of Oceanography, JOSA 47, 499-506.
- Johnson, R. W., W. S. Hering, and J. E. Shields (1989), *Automated Visibility and Cloud Cover Measurements with a Solid-State Imaging System*, University of California, San Diego, Scripps Institution of Oceanography, Marine Physical Laboratory, SIO Ref. 89-7, GL-TR-89-0061M, ADA216906.
- Johnson, R. W., M. E. Karr, and J. R. Varah (1990), *Automated Visibility Measurements with a Horizon Scanning Imager*, University of California, San Diego, Scripps Institution of Oceanography, Marine Physical Laboratory, to be published.
- Shields, J. E. (1989), *Software Documentation: Linearity Processing*, University of California, San Diego, Scripps Institution of Oceanography, Marine Physical Laboratory, Technical Note AV89-056t.